# Pattern formation in weakly damped parametric surface waves

## By WENBIN ZHANG[1] AND JORGE VIÑALS[2]

[1]Department of Chemical Engineering, Massachusetts Institute of Technology, Cambridge, MA 02139, USA

[2]Supercomputer Computations Research Institute, Florida State University, Tallahassee, FL 32306-4052, USA, *and* Department of Chemical Engineering, FAMU-FSU College of Engineering, Tallahassee, FL 31310-6046, USA

We present a theoretical study of nonlinear pattern formation in parametric surface waves for fluids of low viscosity, and in the limit of large aspect ratio. The analysis is based on a quasi-potential approximation to the equations governing fluid motion, followed by a multiscale asymptotic expansion in the distance away from threshold. Close to onset, the asymptotic expansion yields an amplitude equation which is of gradient form, and allows the explicit calculation of the functional form of the cubic nonlinearities. In particular, we find that three-wave resonant interactions contribute significantly to the nonlinear terms, and therefore are important for pattern selection. Minimization of the associated Lyapunov functional predicts a primary bifurcation to a standing wave pattern of square symmetry for capillary-dominated surface waves, in agreement with experiments. In addition, we find that patterns of hexagonal and quasi-crystalline symmetry can be stabilized in certain mixed capillary–gravity waves, even in this case of single-frequency forcing. Quasi-crystalline patterns are predicted in a region of parameters readily accessible experimentally.

## 1. Introduction

The generation of standing waves on the free surface of a fluid layer that is oscillated vertically has been known since the work of Faraday (1831). Recently, there has been renewed experimental interest in Faraday waves as an example of a pattern-forming system. Reasons include the ease of experimentation due to short characteristic time scales (of the order of $10^{-2}$ s), and the ability to reach very large aspect ratios (the ratio of lateral size of the system to the characteristic wavelength of the pattern) of the order of $10^2$. By varying the form of the driving force and by using fluids of different viscosities, a number of interesting phenomena have been observed including the emergence of standing wave patterns of different symmetries near onset (Christiansen, Alstrøm & Levinsen 1992; Fauve *et al.* 1992; Edwards & Fauve 1993, 1994; Müller 1993), secondary instabilities of these patterns when the amplitude of the periodic driving force is increased (Ezerskii, Korotin & Rabinovich 1985; Daudet *et al.* 1995), and spatiotemporal chaotic states at even larger amplitudes of the driving force (Tufillaro, Ramshankar & Gollub 1989; Gollub & Ramshankar 1991; Bosch & van de Water 1993; Bridger *et al.* 1993; Kudrolli & Gollub 1996).

A numerical linear stability analysis of the Faraday wave problem has been carried out by Kumar & Tuckerman (1994) for a laterally infinite fluid layer of arbitrary viscosity. The predicted values of the acceleration threshold and the wavelength at onset are in good agreement with experiments in large aspect ratio systems (see also Bechhoefer *et al.* 1995). In the simpler case of an ideal fluid, a classical linear stability analysis leads to the Mathieu equation for the interface displacement (Benjamin & Ursell 1954). On the other hand, the nonlinear evolution above onset, including pattern selection, secondary instabilities and the transition to spatiotemporal chaos, are not very well understood theoretically. In this paper, we present a weakly nonlinear analysis of Faraday waves driven by a sinusoidal force in the limit of weak dissipation and for a laterally infinite system of infinite depth (or unbounded free surface waves). Our main focus is on pattern selection near onset, and our results are compared to experiments involving fluids of low viscosity, in containers of large depth and aspect ratio.

Many studies of free surface waves in incompressible fluids have focused on the inviscid limit (see, for example, Yuen & Lake 1982; Craik 1985). Viscous dissipation, however, is essential for Faraday waves because it not only sets a threshold value of the driving force, but also affects nonlinear saturation of the parametric instability. For unbounded free surface waves in the limit of weak dissipation, the flow remains potential except in a very thin layer at the free surface (Lamb 1932; Landau & Lifshitz 1959). A common procedure in this limit involves the introduction of the so-called quasi-potential approximation which perturbatively incorporates weak viscous effects by introducing modified boundary conditions for the otherwise potential bulk flow. By performing a formal expansion in the small thickness of the viscous boundary layer, Lundgren & Mansour (1988) derived a set of quasi-potential equations (QPEs) that included nonlinear viscous contributions for the free surface flow of an axially symmetric liquid drop. Ruvinsky *et al.* (1991) later derived a set of QPEs that contain only linear damping terms for two-dimensional free surface waves. In §2, we present QPEs for parametric surface waves including only linear viscous terms. These equations are a direct extension of those of Ruvinsky *et al.* for the two-dimensional case. They can also be derived in a formal expansion similar to that of Lundgren & Mansour (1988) and neglecting nonlinear viscous terms. Such a formal derivation and the expressions for the nonlinear viscous terms can be found in Zhang (1994).

Since we are interested in the surface displacement, but not in the flow field in the fluid interior, additional simplification is achieved by writing the three-dimensional QPEs in a two-dimensional non-local form, that involves flow variables at the free surface alone. Such simplification is possible because the velocity potential satisfies Laplace's equation in the fluid interior, and is determined uniquely when its values on the boundary (the free surface) are known. An outline of the derivation of the weakly nonlinear two-dimensional form of the QPEs is given in §2.2 by using the so-called Dirichlet–Neumann operator (Craig 1989). The projection of the fluid equations onto equations involving the coordinates of the free surface follows the works of Miles (1977), Milder (1977), and Craig (1989) for inviscid gravity waves. These two-dimensional non-local QPEs are our starting point for our weakly nonlinear analysis of parametric surface waves which is presented in §3. Standing wave amplitude equations are derived by using a multiple-scale perturbation expansion. Pattern selection in Faraday waves near onset is discussed in §3.3.

Although the relation between our results and earlier theoretical work on Faraday waves is discussed in more detail below, we note here the two important studies

addressing the weakly nonlinear regime above onset by Milner (1991), and Miles (1993, 1994). They obtained amplitude equations for inviscid flow, and then introduced weak viscous effects by adding damping terms directly to the amplitude equations from an energy balance consideration. The resulting amplitude equations differ from ours in several respects, hence our results differ qualitatively from theirs, as discussed in §3.

## 2. Quasi-potential equations for free surface waves

We consider a reference state in which a quiescent and incompressible Newtonian liquid of density $\rho$ and kinematic viscosity $v$ occupies the $z < 0$ half-space, and a gas of negligible density occupies the $z > 0$ half-space. The gas phase is also assumed to have a uniform and constant pressure field $p_0$. Under these conditions, the velocity distribution of the gas phase may be allowed to remain unknown and we can write the governing equations for the liquid phase only. Such a liquid–gas interface is usually called the *free* surface of a liquid (Batchelor 1967). The governing equations for the velocity field $\boldsymbol{v}(x, y, z, t)$ are for $-\infty < z < h(x, y, t)$, where $z = h(x, y, t)$ is the instantaneous location of the free surface,

$$\nabla \cdot \boldsymbol{v} = 0, \tag{2.1}$$

$$\partial_t \boldsymbol{v} + (\boldsymbol{v} \cdot \nabla)\boldsymbol{v} = -\frac{1}{\rho}\nabla p + v\nabla^2 \boldsymbol{v} + g(t)\hat{\boldsymbol{z}}, \tag{2.2}$$

where $\hat{\boldsymbol{z}}$ is the unit vector in the positive $z$-direction, and $g(t) = -g_0 - g_z(t)$ with $g_0$ a constant gravitational acceleration, and $g_z(t)$ the effective acceleration caused by the vertical oscillation of the fluid in the Faraday experiments. The boundary conditions at the free surface are

$$\partial_t h/(1 + (\nabla h)^2)^{1/2} = \boldsymbol{v} \cdot \hat{\boldsymbol{n}}, \tag{2.3}$$

$$\hat{\boldsymbol{a}} \cdot \boldsymbol{\tau} \cdot \hat{\boldsymbol{n}} \equiv 2\rho v \hat{\boldsymbol{a}} \cdot \mathbf{e} \cdot \hat{\boldsymbol{n}} = 0, \tag{2.4}$$

$$\hat{\boldsymbol{b}} \cdot \boldsymbol{\tau} \cdot \hat{\boldsymbol{n}} \equiv 2\rho v \hat{\boldsymbol{b}} \cdot \mathbf{e} \cdot \hat{\boldsymbol{n}} = 0, \tag{2.5}$$

$$p - \hat{\boldsymbol{n}} \cdot \boldsymbol{\tau} \cdot \hat{\boldsymbol{n}} \equiv p - 2\rho v \hat{\boldsymbol{n}} \cdot \mathbf{e} \cdot \hat{\boldsymbol{n}} = p_0 + \Gamma \kappa, \tag{2.6}$$

with boundary condition

$$\boldsymbol{v} = 0 \quad \text{as} \quad z \to -\infty, \tag{2.7}$$

where $\hat{\boldsymbol{a}}(x, y, t)$ and $\hat{\boldsymbol{b}}(x, y, t)$ are two tangential unit vectors on the free surface, and $\hat{\boldsymbol{n}}(x, y, t) = (-h_x, -h_y, 1)/(1 + (\nabla h)^2)^{1/2}$ is the unit normal vector of the free surface pointing away from the liquid. $\Gamma$ is the surface tension, $\kappa$ is the mean curvature of the free surface, which is given by $\kappa = \nabla \cdot \hat{\boldsymbol{n}}$, and $\boldsymbol{\tau} = 2\rho v \mathbf{e}$ is the viscous stress tensor, where $\mathbf{e}$ is the rate of strain tensor with Cartesian components ($i, j = x, y, z$)

$$(\mathbf{e})_{ij} = \frac{1}{2}\left(\frac{\partial v_i}{\partial x_j} + \frac{\partial v_j}{\partial x_i}\right). \tag{2.8}$$

The equations governing fluid motion can be simplified in the limit of weak viscous dissipation. In this case, a thin viscous boundary layer, also known as the vortical layer, occurs near the free surface as a result of the non-zero irrotational shear stresses. This small irrotational shear stress drags a thin viscous layer of

rotational fluid along, causing a small modification in the velocity field which is required in order to satisfy the zero-shear-stress boundary conditions ((2.4) and (2.5)). Since the free surface vortical layer is thin, the basic idea of the quasi-potential approximation is to consider pure potential flow in the bulk that satisfies effective boundary conditions on the moving surface to account for weak viscous effects.

### 2.1. *Three-dimensional form of the quasi-potential equations*

Let $\phi(x, y, z, t)$ be the velocity potential for the bulk potential flow. As a direct extension of the QPEs of Ruvinsky *et al.* (1991) for two-dimensional surface waves, the governing equations for unbounded three-dimensional surface waves are

$$\nabla^2 \phi(x, y, z, t) = 0 \quad \text{for} \quad z < h(x, y, t), \tag{2.9}$$

with boundary conditions at the free surface $z = h(x, y, t)$

$$\partial_t h + \nabla \phi \cdot \nabla h = \partial_z \phi + W(x, y, t), \tag{2.10}$$

$$\partial_t + \tfrac{1}{2}(\nabla \phi)^2 - g(t)h + 2v\frac{\partial^2 \phi}{\partial z^2} = \Gamma \kappa, \tag{2.11}$$

$$\partial_t W(x, y, t) = 2v\left(\partial_{xx} + \partial_{yy}\right)\partial_z \phi, \tag{2.12}$$

and

$$\partial_z \phi \to 0 \quad \text{as} \quad z \to -\infty, \tag{2.13}$$

where $W(x, y, t)$ is the $z$-component (or the linearized normal component) of the rotational part of the velocity field at the free surface. The viscous contribution in (2.11) is related to the normal stress of the irrotational velocity component. We note that only linear viscous (damping) terms are retained in the above set of equations, which we shall refer to as LDQPEs. Nonlinear viscous contributions can be obtained by using a formal perturbation expansion, similar to that of Lundgren & Mansour (1988), of (2.1)–(2.7) in the small thickness of the viscous boundary layer at the free surface. Details of the expansion can be found in Zhang (1994). These nonlinear viscous terms for three-dimensional waves are, however, algebraically too complicated to be included in our analysis. We note that neglecting nonlinear viscous contributions in the above equations is an uncontrolled approximation, motivated by the small viscosity of the fluid. Whether the LDQPEs are a good approximation for weakly damped parametric surface waves near onset is one of the central issues of this paper. Based on our analytical results of the LDQPEs in §3, and the comparison of these results with experiments, we conclude that the LDQPEs do provide a quite good description of weakly damped and weakly nonlinear Faraday waves. This seems to indicate that the role of nonlinear viscous terms in the QPEs is not significant for pattern formation in weakly damped Faraday waves close to onset.

The $z$-component of the rotational part of the velocity $W(x, y, t)$ can be eliminated. From (2.10) and (2.12), we have

$$\partial_t W = 2v(\partial_{xx} + \partial_{yy})\partial_t h + 2v(\partial_{xx} + \partial_{yy})(\nabla \phi \cdot \nabla h - W). \tag{2.14}$$

We note that $v\nabla \phi \cdot \nabla h$ is a nonlinear viscous term, and thus negligible within the approximation. Since $W$ is of $O(v)$, the term $vW$ in the above equation is of $O(v^{-2})$, and is negligible in the weakly damped limit. Therefore we have $\partial_t(W - 2v\nabla^2 h) = 0$, or

$$W(x, y, t) = 2v\nabla^2 h(x, y, t) + W_0 - 2v\nabla^2 h_0, \tag{2.15}$$

where $h_0$ and $W_0$ are initial conditions for $h$ and $W$ respectively. By considering fluid motion starting from rest, we can set $W_0 = 0$. Also since we are interested in nonlinear pattern formation from a nearly flat surface, $h_0$ is a small quantity. Although the term $2v\nabla^2 h_0$ might influence the linear growth, it is certainly negligible for nonlinear finite-amplitude states. Thus the boundary conditions at $z = h(x, y, t)$ ((2.10) and (2.11)) now read

$$\partial_t h = 2v\nabla^2 h - \nabla_\perp \phi \cdot \nabla h + \partial_z \phi, \tag{2.16}$$

$$\partial_t \phi = 2v\nabla_\perp^2 \phi - \tfrac{1}{2}(\nabla\phi)^2 + g(t)h - \Gamma \kappa, \tag{2.17}$$

where $\nabla_\perp = \partial_x \hat{\boldsymbol{x}} + \partial_y \hat{\boldsymbol{y}}$.

### 2.2. *Two-dimensional non-local form of the quasi-potential equations*

For weakly nonlinear surface waves, the three-dimensional QPEs can be further simplified by recasting them in a form that involves only the flow variables on the free surface. Since the velocity potential $\phi$ satisfies Laplace's equation in the bulk, it is possible to rewrite the LDQPEs as integro-differential equations involving variables at the free surface only. We then expand the resulting equations to third order in the wave steepness. Such a two-dimensional non-local formulation has been derived by Miles (1977), Milder (1977), Craig (1989), and Craig & Sulem (1993) for un-forced inviscid gravity waves. We extend their approach in this section to parametrically forced weakly damped capillary–gravity waves.

Let $\boldsymbol{x} = (x, y)$, and define the surface velocity potential $\Phi(\boldsymbol{x}, t)$ as $\Phi(\boldsymbol{x}, t) = \phi(\boldsymbol{x}, h(\boldsymbol{x}, t), t)$. Then (2.16) and (2.17) can be rewritten as

$$\partial_t h = 2v\nabla^2 h + (1 + (\nabla h)^2)^{1/2}\partial_n \phi, \tag{2.18}$$

$$\partial_t \Phi = 2v\nabla^2 \Phi - \tfrac{1}{2}(\nabla\Phi)^2 + \frac{\left[(1 + (\nabla h)^2)^{1/2}\partial_n \phi + \nabla\Phi \cdot \nabla h\right]^2}{2\left[1 + (\nabla h)^2\right]}$$
$$+ g(t)h + \frac{\Gamma}{\rho}\nabla \cdot \left(\frac{\nabla h}{(1 + (\nabla h)^2)^{1/2}}\right), \tag{2.19}$$

where $\partial_n \phi = \hat{\boldsymbol{n}} \cdot (\nabla_\perp + \partial_z \hat{\boldsymbol{z}})\phi$. We note that except for the normal derivative $\partial_n \phi$, all other variables only depend on the two-dimensional coordinate $\boldsymbol{x}$. Since $\phi$ is a harmonic function, the normal derivative $\partial_n \phi$ at the boundary is related to the value of $\phi$ at the boundary. One such relation is given by the Dirichlet–Neumann operator $\hat{\mathcal{G}}(h)$, which takes boundary values for a harmonic function and returns its normal derivative at the boundary with a metric pre-factor (Craig 1989; Craig & Sulem 1993):

$$\hat{\mathcal{G}}(h)\Phi(\boldsymbol{x}, t) = (1 + (\nabla h)^2)^{1/2}\partial_n \phi. \tag{2.20}$$

We note that $\hat{\mathcal{G}}(h)$ is a linear operator for $\Phi(\boldsymbol{x}, t)$ and depends on the shape of the free surface $z = h(\boldsymbol{x}, t)$ non-locally.

An important property of $\hat{\mathcal{G}}(h)$ is that it has a computable Taylor expansion in powers of the surface displacement $h(\boldsymbol{x}, t)$ and its spatial derivatives at $h(\boldsymbol{x}, t) = 0$. This Taylor expansion of $\hat{\mathcal{G}}(h)$ is useful for studying the weakly nonlinear dynamics of surface waves since only the first a few terms in the expansion, e.g. up to third order in $h(\boldsymbol{x}, t)$, need to be evaluated. The Taylor expansion of $\hat{\mathcal{G}}(h)$ up to $O(h^3)$ reads

$$\hat{\mathcal{G}}(h)\Phi(\boldsymbol{x},t) = \hat{\mathcal{D}}\Phi - \nabla \cdot (h\nabla\Phi) - \hat{\mathcal{D}}(h\hat{\mathcal{D}}\Phi) + \hat{\mathcal{D}}\left[h\hat{\mathcal{D}}(h\hat{\mathcal{D}}\Phi) + \tfrac{1}{2}h^2\nabla^2\Phi\right]$$

$$+\tfrac{1}{2}\nabla^2(h^2\hat{\mathcal{D}}\Phi) - \nabla^2\left[\tfrac{1}{2}h^2\hat{\mathcal{D}}(h\hat{\mathcal{D}}\Phi) + \tfrac{1}{3}h^3\nabla^2\Phi\right]$$

$$-\hat{\mathcal{D}}\left[h\hat{\mathcal{D}}(h\hat{\mathcal{D}}(h\hat{\mathcal{D}}\Phi)) + \tfrac{1}{2}h^2\nabla^2(h\hat{\mathcal{D}}\Phi) - \tfrac{1}{6}h^3\nabla^2(\hat{\mathcal{D}}\Phi) + \tfrac{1}{2}h\hat{\mathcal{D}}(h^2\nabla^2\Phi)\right], \quad (2.21)$$

where $\hat{\mathcal{D}}$ is a linear Fourier-integral operator and is defined for an arbitrary function $u(\boldsymbol{x})$ by

$$\hat{\mathcal{D}}u(\boldsymbol{x}) = \int_{-\infty}^{\infty} |\boldsymbol{k}|\hat{u}(\boldsymbol{k})\exp(\mathrm{i}\boldsymbol{k}\cdot\boldsymbol{x})\mathrm{d}\boldsymbol{k}$$

where $\hat{u}(\boldsymbol{k})$ is the Fourier transform of $u(\boldsymbol{x})$. The operator $\hat{\mathcal{D}}$ is also non-local and is sometimes written as $\hat{\mathcal{D}} = (-\nabla^2)^{1/2}$. By substituting the expansion for the Dirichlet–Neumann operator $\hat{\mathcal{G}}(h)$ into the boundary conditions, and consistently keeping only terms up to the third order in $h$ and/or $\Phi$, we have

$$\partial_t h(\boldsymbol{x},t) = 2v\nabla^2 h + \hat{\mathcal{D}}\Phi - \nabla \cdot (h\nabla\Phi) + \tfrac{1}{2}\nabla^2(h^2\hat{\mathcal{D}}\Phi)$$

$$-\hat{\mathcal{D}}(h\hat{\mathcal{D}}\Phi) + \hat{\mathcal{D}}\left[h\hat{\mathcal{D}}(h\hat{\mathcal{D}}\Phi) + \tfrac{1}{2}h^2\nabla^2\Phi\right], \quad (2.22)$$

$$\partial_t\Phi(\boldsymbol{x},t) = 2v\nabla^2\Phi + g(t)h + \frac{\Gamma}{\rho}\nabla^2 h + \tfrac{1}{2}\left(\hat{\mathcal{D}}\Phi\right)^2 - \tfrac{1}{2}(\nabla\Phi)^2$$

$$-(\hat{\mathcal{D}}\Phi)\left[h\nabla^2\Phi + \hat{\mathcal{D}}(h\hat{\mathcal{D}}\Phi)\right] - \frac{\Gamma}{2\rho}\nabla \cdot \left(\nabla h(\nabla h)^2\right). \quad (2.23)$$

Consideration of higher-order terms is certainly not a difficulty in this formulation, but most of the phenomena in Faraday waves near onset should be explained within a framework that includes up to third-order nonlinearities. Equations (2.22) and (2.23) are two-dimensional, and they are the starting point for the analytical asymptotic analysis presented below, and for extensive numerical studies that will be reported elsewhere (a short summary of both analytical and numerical results can be found in Zhang & Viñals 1996).

Finally, we note that the incompressibility condition (2.1) implies that the average level of the surface displacement $h(\boldsymbol{x},t)$ is constant,

$$\int_S h(\boldsymbol{x},t)\mathrm{d}\boldsymbol{x} = \text{constant}. \quad (2.24)$$

It is easy to see that $\int_S h(\boldsymbol{x},t)\mathrm{d}\boldsymbol{x}$ is indeed a constant of motion for (2.22).

Before we proceed any further, it is useful to discuss the dissipation function approach used by other authors to obtain dissipative contributions to the equation of motion for weakly damped waves, and compare it with the quasi-potential approximation. As we show below, both methods differ in the linear viscous terms in the dynamical equations even though, by construction, they give the same (correct) rate of decay of the energy for linear surface waves. As a consequence, is seems to us that nonlinear viscous terms obtained from an energy balance for the inviscid amplitude equation may not be reliable.

It is well known that the irrotational surface wave problem in an inviscid fluid can be written in a Hamiltonian form (Zakharov 1968; Miles 1977). The governing equations for irrotational surface waves can be written in this case as

$$\partial_t h(\boldsymbol{x},t) = \frac{\delta H}{\delta\Phi(\boldsymbol{x},t)}, \quad (2.25)$$

$$\partial_t \Phi(\boldsymbol{x}, t) = -\frac{\delta H}{\delta h(\boldsymbol{x}, t)}, \tag{2.26}$$

where $h(\boldsymbol{x}, t)$ and $\Phi(\boldsymbol{x}, t)$ are the generalized coordinate and momentum respectively, and the Hamiltonian $H$ is given by

$$H = \iint \mathrm{d}\boldsymbol{x} \left[ \frac{1}{2} \int_{-\infty}^{h(\boldsymbol{x},t)} \mathrm{d}z \left( (\nabla_\perp \phi)^2 + (\partial_z \phi)^2 \right) + \tfrac{1}{2} g(t) h^2 + \Gamma \left( [1 + (\nabla h)^2]^{1/2} - 1 \right) \right]. \tag{2.27}$$

This Hamiltonian formulation (or equivalently the corresponding Lagrangian formulation) offers a natural way to incorporate the effects of viscous damping by adding a dissipation function. This is done by modifying the equation for the generalized momentum $\Phi(\boldsymbol{x}, t)$,

$$\partial_t \Phi(\boldsymbol{x}, t) = -\frac{\delta H}{\delta h(\boldsymbol{x}, t)} + Q(h(\boldsymbol{x}, t), \Phi(\boldsymbol{x}, t)), \tag{2.28}$$

where $Q(h, \Phi)$ is a dissipative or damping force, not invariant under time reversal, and often of phenomenological nature. In the case of Faraday waves, the dissipation function $Q(h, \Phi)$ has been determined by equating the rate of energy loss in this near-Hamiltonian formulation,

$$\frac{\mathrm{d}H}{\mathrm{d}t} - \frac{\partial H}{\partial t} = \iint \mathrm{d}\boldsymbol{x} \, Q(h, \Phi) \partial_t h, \tag{2.29}$$

to the decay rate of the total energy for potential flow (Landau & Lifshitz 1959),

$$\iint \mathrm{d}\boldsymbol{x} \, Q(h, \Phi) \partial_t h = -v \iint \mathrm{d}\boldsymbol{x} \int_{-\infty}^{h(\boldsymbol{x},t)} \nabla^2 (\nabla \phi)^2. \tag{2.30}$$

It is easy to show that the linear part of $Q$ depends only on $\Phi(\boldsymbol{x}, t)$, and is given by

$$Q(h, \Phi) = 4v \nabla^2 \Phi(\boldsymbol{x}, t) + \text{nonlinear terms}. \tag{2.31}$$

If we consider the linear approximation for $Q$, (2.26) is modified by the addition of a viscous damping term $4v \nabla^2 \Phi(\boldsymbol{x}, t)$ to the right-hand side, while (2.25) remains unchanged.

However, in the quasi-potential approximation, viscous damping terms appear in both the $\partial_t h$ equation and the $\partial_t \Phi$ equation ((2.22) and (2.23)). This difference has important implications for the standing wave amplitude equations to be derived in §3. Recall that the viscous correction term in the $\partial_t h$ equation is related to the rotational component of the velocity field at the fluid surface, while the viscous correction term in the $\partial_t \Phi$ equation is related to the normal stress of the irrotational component.

For linear surface waves, both approaches give the same dynamical equation for a Fourier mode $\hat{h}_k(t)$ of $h(\boldsymbol{x}, t)$,

$$\partial_{tt} \hat{h}_k(t) + 4v k^2 \partial_t \hat{h}_k(t) + \left( \frac{\Gamma k^3}{\rho} + g_0 k + k g_z(t) \right) \hat{h}_k(t) = 0. \tag{2.32}$$

Thus, the decay rate of the total energy for linear surface waves is the same for the two approaches, as expected.

Since the calculation of the dissipation function $Q$ can be carried out for the nonlinear terms as well, it would appear that the dissipative function approach is a natural way to incorporate nonlinear viscous terms order by order. However, since the dissipation function approach does not give the correct linear viscous terms ((2.28) and (2.31) lead to a linear viscous term in the equation for $\partial_t \Phi$ equal to $4v \nabla^2 \Phi$,

whereas the linear viscous term in (2.23) is only $2\nu\nabla^2\Phi$), there does not seem to be any *a priori* reason to trust nonlinear viscous terms.

## 3. Weakly nonlinear analysis

Standing wave patterns of square symmetry are observed near onset in Faraday experiments on weakly viscous fluids, in containers of large lateral size, and with single-frequency sinusoidal forcing (Faraday 1831; Rayleigh 1883; Lang 1962; Ezerskii *et al.* 1985; Tufillaro *et al.* 1989; Ciliberto *et al.* 1991; Christiansen *et al.* 1992; Bosch & van de Water 1993; Edwards & Fauve 1993, 1994; Müller 1993). We derive next a set of coupled standing wave amplitude equations valid near onset that can accommodate patterns of arbitrary symmetry on a two-dimensional surface. The standing wave amplitude equations that we will obtain are of gradient form, and thus minimization of the resulting Lyapunov functional determines the symmetry of the most-stable standing wave state. Our derivation of the standing amplitude equations has three novel features. The first one is the different starting point for the asymptotic expansion. It is based on the LDQPEs described above. Second, we note that there are two independent small parameters in this system, namely the reduced dimensionless driving amplitude $\varepsilon$, which is also the distance away from threshold, and the viscous damping parameter $\gamma$ (to be defined below). A double perturbative expansion for these two small parameters is necessary. Solutions of the linearized quasi-potential equations are obtained by performing a perturbative expansion for the small damping parameter or the driving amplitude $f$ (to be defined below). The linear solutions contain the primary mode of the fluid surface with a frequency of half the driving frequency as well as its higher-harmonics. These higher-harmonic terms are proportional to the driving amplitude $f$ or its powers ($f^n$, with $n = 2, 3, \ldots$). The nonlinear interaction of these higher-harmonic terms with the primary mode provides a novel *amplitude-limiting effect* for the parametric surface wave system. This effect is important for the nonlinear saturation of the surface wave amplitude in weakly dissipative systems.

The third feature is related to three-wave resonant interactions in capillary–gravity surface waves. Although quadratic terms are prohibited by symmetry in the standing wave amplitude equations that we derive, three-wave resonance (triad resonance) plays a crucial role in pattern selection. Both three- and four-wave resonant interactions among capillary–gravity waves are well known and well studied. The importance of three-wave resonant interactions to pattern selection in Faraday waves, however, has been largely overlooked. As we show later, the resonant interactions between two linearly unstable standing wave modes and a linearly stable wave mode strongly affect four-wave nonlinear interactions, and thus the coefficient of third-order nonlinear terms in the amplitude equations.

Previous theoretical work by Milner (1991) involved the derivation of a set of coupled travelling wave amplitude equations for inviscid parametric surface waves, to which viscous damping terms were added by an energy balance consideration, equivalent to the dissipation function approach described above. He concluded that nonlinear viscous damping terms in the dissipation function play a major role in pattern selection. We disagree with his conclusion for four reasons. (i) As discussed earlier, the dissipation function approach does not give the correct linear viscous terms, so it is doubtful that it will introduce the correct nonlinear damping terms; (ii) linear viscous terms in the fluid equations can contribute to nonlinear damping terms in the amplitude equations, while such contribution is absent

in Milner's phenomenological consideration of viscous effects; (iii) an amplitude-limiting effect of the driving force did not appear in Milner's analysis since he used a zeroth-order linear solution for the parametric instability; and (iv) Milner did obtain triad resonant interactions in his calculation, but by not taking them into account explicitly, he overlooked their effect on pattern selection. As was recently suggested by Edwards & Fauve (1994), we will show that triad resonant interactions play an important role in pattern formation of Faraday waves in weakly viscous fluids.

### 3.1. *Solutions of the linearized equations*

As is well known, the linearized problem of parametric surface waves can be reduced to the damped Mathieu equation, and the Faraday instability corresponds to the subharmonic resonance of the equation. For the case of a sinusoidal driving force, the effective acceleration $g(t)$ in (2.22) and (2.23) can be written as $g(t) = -g_0 - g_z \sin \Omega t$, where $g_0$ is the constant acceleration due to gravity, and $\Omega$ and $g_z$ are the angular frequency and the amplitude of the driving force respectively. We now choose $2/\Omega \equiv 1/\omega_0$ as the unit of time and $1/k_0$ as the unit of length with $k_0$ defined by $\omega_0^2 = g_0 k_0 + (\Gamma/\rho)k_0^3$. We also choose the unit for the surface velocity potential $\Phi$ to be $\omega_0/k_0^2$. We further define a dimensionless linear damping coefficient $\gamma = 2vk_0^2/\omega_0$, $G_0 = g_0 k_0/\omega_0^2$, $\Gamma_0 = \Gamma k_0^3/(\rho\omega_0^2)$, and the dimensionless driving amplitude $f = g_z k_0/(4\omega_0^2)$. Note that $G_0 + \Gamma_0 = 1$ by definition.

By linearizing the QPEs and boundary conditions ((2.22) and (2.23)) with respect to the surface displacement $h$, and the surface velocity potential $\Phi$, and taking the Fourier transform with respect to the spatial coordinate, one obtains in a standard way

$$\partial_{tt}\hat{h}_k + 2\gamma k^2 \partial_t \hat{h}_k + \left(G_0 k + \Gamma_0 k^3 + \gamma^2 k^4 + 4fk \sin 2t\right)\hat{h}_k = 0, \tag{3.1}$$

$$k\hat{\Phi}_k = \partial_t \hat{h}_k + \gamma k^2 \hat{h}_k. \tag{3.2}$$

Equation (3.1) is the damped Mathieu equation for $\hat{h}_k$. We now seek analytical solutions of the above equations perturbatively. We introduce a small parameter $\eta$ ($\eta \ll 1$) such that $\gamma = \gamma_0\eta$, and $f = f_0\eta$, where $\gamma_0$ and $f_0$ are assumed to be of $O(1)$ (as we shall see later, $f = \gamma$ at onset). For weakly dissipative fluids, i.e. $\gamma \ll 1$, and to be consistent with the quasi-potential approximation discussed in the previous section, we will neglect the term proportional to $\gamma^2$ in (3.1). At subharmonic resonance, we have $\omega^2(k) \equiv G_0 k + \Gamma_0 k^3 = 1$, which of course implies $k = 1$ (note that $G_0 + \Gamma_0 = 1$ by definition). We then consider an expansion for the wavenumber $k$ near subharmonic resonance as $k = 1 + \Delta k\eta + \dots$. Above (and near) the onset of subharmonic resonance, we expect the amplitudes of $\hat{h}_k$ to grow in time but in a slower time scale than that for the subharmonic oscillation. In the following we assume that the slow time is $T = \eta t$, and seek solutions perturbatively as power series in $\eta$:

$$\hat{h}_k = \hat{h}_k^{(0)}(t, T) + \eta \hat{h}_k^{(1)}(t, T) + \dots,$$

$$\hat{\Phi}_k = \hat{\Phi}_k^{(0)}(t, T) + \eta \hat{\Phi}_k^{(1)}(t, T) + \dots.$$

At $O(\eta^0)$, one has

$$\hat{h}_k^{(0)}(t, T) = A_k(T)\cos t + B_k(T)\sin t,$$

$$\hat{\Phi}_k^{(0)}(t, T) = -A_k(T)\sin t + B_k(T)\cos t,$$

where $A_k(T)$ and $B_k(T)$ are arbitrary functions. At $O(\eta^1)$, a standard solvability

condition appears,

$$\partial_T A = (f_0 - \gamma_0)A + \tfrac{1}{2}(G_0 + 3\Gamma_0)\Delta k B, \tag{3.3}$$

$$\partial_T B = -(f_0 + \gamma_0)B - \tfrac{1}{2}(G_0 + 3\Gamma_0)\Delta k A. \tag{3.4}$$

By substituting $A$ and $B \propto e^{\sigma t}$, one finds

$$\sigma_\pm = -\gamma_0 \pm \left[ f_0^2 - \left( \tfrac{1}{2}\Delta k(G_0 + 3\Gamma_0) \right)^2 \right]^{1/2}. \tag{3.5}$$

Exactly at subharmonic resonance ($k = 1$ or $\Delta k = 0$), the growing mode $M_+ \propto A$ and the decaying mode $M_- \propto B$. In this case, the linearly growing eigenmode above onset is given by

$$h(\boldsymbol{x}, t) = \left( \cos t + \tfrac{1}{4}f \sin 3t + \ldots \right) \sum_{j=1}^{N} \left[ A_j(t) \exp\left( i\hat{\boldsymbol{k}}_j \boldsymbol{x} \right) + \text{c.c.} \right], \tag{3.6}$$

$$\Phi(\boldsymbol{x}, t) = \left( -\sin t + f \cos t + \tfrac{3}{4}f \cos 3t + \ldots \right) \sum_{j=1}^{N} \left[ A_j(t) \exp\left( i\hat{\boldsymbol{k}}_j \boldsymbol{x} \right) + \text{c.c.} \right], \tag{3.7}$$

where we have assumed that the standing waves consist of an arbitrary discrete set of wavevectors in the two-dimensional space. When $f = \gamma$ (at onset), (3.6) and (3.7) are the linear neutral solutions, which is the basis of a weakly nonlinear analysis for our problem. It is important to note at this point that we have kept in the linear solution terms proportional to $f$ (or $\gamma$ since $f = \gamma$ at onset). These terms will be crucial for obtaining the correct cubic term in the amplitude equations, and had not been included in previous studies. Terms proportional to higher harmonics do not contribute to the standing wave amplitude equations to the order considered.

### 3.2. *Standing wave amplitude equations*

We seek nonlinear standing wave solutions of Faraday waves near onset ($\varepsilon \equiv (f - \gamma)/\gamma \ll 1$) in this subsection. We expand the two-dimensional quasi-potential equations ((2.22) and (2.23)) consistently in $\varepsilon^{1/2}$ with multiple time scales

$$h(\boldsymbol{x}, t, T) = \varepsilon^{1/2} h_1(\boldsymbol{x}, t, T) + \varepsilon h_2 + \varepsilon^{3/2} h_3 + \ldots, \tag{3.8}$$

$$\Phi(\boldsymbol{x}, t, T) = \varepsilon^{1/2} \Phi_1(\boldsymbol{x}, t, T) + \varepsilon \Phi_2 + \varepsilon^{3/2} \Phi_3 + \ldots, \tag{3.9}$$

where the slow time scale $T = \varepsilon t$, and is not related to the slow time in the previous subsection. The scaling of the amplitudes and the slow time $T$ with $\varepsilon$ is formally determined by the ultimate consistency of the expansion, and in particular by the balance of terms in the final form of the standing wave amplitude equation (3.34). We define the following linear operator:

$$\mathscr{L} \equiv \begin{pmatrix} \partial_t - \gamma\nabla^2 & -\hat{\mathscr{D}} \\ G_0 - \Gamma_0\nabla^2 + 4\gamma\sin 2t & \partial_t - \gamma\nabla^2 \end{pmatrix}. \tag{3.10}$$

On substituting (3.8) and (3.9) into the QPEs we have at $O(\varepsilon^{1/2})$,

$$\mathscr{L} \begin{pmatrix} h_1 \\ \Phi_1 \end{pmatrix} = 0.$$

The above equation is the same as the linearized quasi-potential equations discussed in the last section except the driving amplitude $f$ is replaced by the damping coefficient

$\gamma$. Thus, the solutions for $h_1$ and $\Phi_1$ are just the linear solutions found in the last subsection. For simplicity, we will neglect the linearly stable mode $B$ of the linear solutions. Then, $h_1$ and $\Phi_1$ are the linear neutral solutions

$$h_1 = \left(\cos t + \tfrac{1}{4}\gamma \sin 3t\right) \sum_{j=1}^{N} \left[A_j(T) \exp\left(\mathrm{i}\hat{\boldsymbol{k}}_j \cdot \boldsymbol{x}\right) + \text{c.c.}\right], \tag{3.11}$$

$$\Phi_1 = \left(-\sin t + \gamma \cos t + \tfrac{3}{4}\gamma \cos 3t\right) \sum_{j=1}^{N} \left[A_j(T) \exp\left(\mathrm{i}\hat{\boldsymbol{k}}_j \cdot \boldsymbol{x}\right) + \text{c.c.}\right]. \tag{3.12}$$

At $O(\varepsilon)$, we have

$$\mathcal{L}\begin{pmatrix} h_2 \\ \Phi_2 \end{pmatrix} = \begin{pmatrix} -\nabla \cdot (h_1 \nabla \Phi_1) - \hat{\mathcal{D}}\left(h_1 \hat{\mathcal{D}} \Phi_1\right) \\ \tfrac{1}{2}(\hat{\mathcal{D}}\Phi_1)^2 - \tfrac{1}{2}(\nabla \Phi_1)^2 \end{pmatrix}. \tag{3.13}$$

The above equation represents two coupled equations for $h_2$ and $\Phi_2$. It is easy to obtain an independent equation for $h_2$ from (3.13), which reads

$$\partial_{tt}h_2 - 2\gamma\nabla^2\partial_t h_2 + (G_0 - \Gamma_0\nabla^2)\hat{\mathcal{D}}h_2 + 4\gamma h_2 \sin 2t$$

$$= \tfrac{1}{2}\hat{\mathcal{D}}\left[(\hat{\mathcal{D}}\Phi_1)^2 - (\nabla\Phi_1)^2\right] + \left(\gamma\nabla^2 - \partial_t\right)\left[\nabla \cdot (h_1\nabla\Phi_1) + \hat{\mathcal{D}}\left(h_1\hat{\mathcal{D}}\Phi_1\right)\right]$$

$$= \sum_{j,l=1}^{N}\left\{\frac{1+c_{jl}}{4}[2(1+c_{jl})]^{1/2} - \cos 2t\left[1 + c_{jl} - \frac{3-c_{jl}}{4}[2(1+c_{jl})]^{1/2}\right]\right.$$

$$\left. -\gamma\sin 2t\left[(\tfrac{5}{2} + c_{jl})\left(1 + c_{jl} - [2(1+c_{jl})]^{1/2}\right) + \frac{1+c_{jl}}{8}[2(1+c_{jl})]^{1/2}\right]\right\}$$

$$\times\left[A_j A_l \exp\left(\mathrm{i}(\hat{\boldsymbol{k}}_j + \hat{\boldsymbol{k}}_l)\cdot\boldsymbol{x}\right) + \text{c.c.}\right]$$

$$+\sum_{j,l=1}^{N}\left\{\frac{1-c_{jl}}{4}[2(1-c_{jl})]^{1/2} - \cos 2t\left[1 - c_{jl} - \frac{3+c_{jl}}{4}[2(1-c_{jl})]^{1/2}\right]\right.$$

$$\left. -\gamma\sin 2t\left[(\tfrac{5}{2} - c_{jl})\left(1 - c_{jl} - [2(1-c_{jl})]^{1/2}\right) + \frac{1-c_{jl}}{8}[2(1-c_{jl})]^{1/2}\right]\right\}$$

$$\times\left[A_j A_l^* \exp\left(\mathrm{i}(\hat{\boldsymbol{k}}_j - \hat{\boldsymbol{k}}_l)\cdot\boldsymbol{x}\right) + \text{c.c.}\right] + \dots, \tag{3.14}$$

where $c_{jl} \equiv \cos\theta_{jl} = \hat{\boldsymbol{k}}_j \cdot \hat{\boldsymbol{k}}_l$ and we have neglected terms that are proportional to $\gamma^2$. Note that there are no terms on the right-hand side proportional to $\cos t$ or $\sin t$ that would introduce a secular variation in the solution. Therefore, there is no solvability condition for the amplitudes $A_j$ at this order. There are, however, resonant interactions due to certain terms on the right-hand side.

The particular solution $h_2$ of (3.14) can be written as

$$h_2 = \sum_{j,l=1}^{N}\left\{H_{jl}(t)\left[A_j A_l \exp\left(\mathrm{i}(\hat{\boldsymbol{k}}_j + \hat{\boldsymbol{k}}_l)\cdot\boldsymbol{x}\right) + \text{c.c.}\right]\right.$$

$$\left. + H_{j,-l}(t)\left[A_j A_l^* \exp\left(\mathrm{i}(\hat{\boldsymbol{k}}_j - \hat{\boldsymbol{k}}_l)\cdot\boldsymbol{x}\right) + \text{c.c.}\right]\right\}, \tag{3.15}$$

where $H_{jl}(t)$ is an unknown function to be determined, and $H_{j,-l}$ is defined by
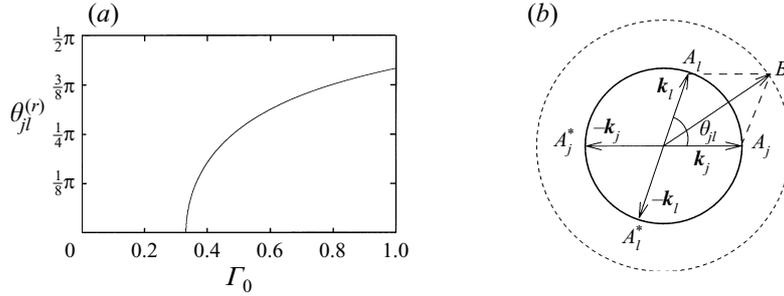
FIGURE 1. Triad resonant interaction in parametric surface waves. (*a*) The angle $\theta_{jl}^{(r)}$ as a function of $\Gamma_0$. (*b*) The mode $B$ will resonate with the quadratic interaction of the standing waves $A_j$ and $A_l$ when $\theta_{jl} = \theta_{jl}^{(r)}$.

replacing $c_{jl}$ with $c_{j,-l}$ in $H_{jl}$. On substituting the above form for $h_2$ into (3.14), we have the following equation for $H_{jl}(t)$:

$$\partial_{tt}H_{jl} + 2\gamma(2(1 + c_{jl}))^{1/2}\partial_t H_{jl} + [G_0 + 2\Gamma_0(1 + c_{jl})](2(1 + c_{jl}))^{1/2}H_{jl}$$
$$= F_{jl}^{(1)}\cos 2t + F_{jl}^{(2)}\sin 2t + \ldots, \qquad (3.16)$$

where $F_{jl}^{(1)}$ and $F_{jl}^{(2)}$ are proportional to $A_jA_l$. Only terms that are relevant to the resonance are written out on the right-hand side of (3.16). Equation (3.16) looks very much like the equation for an additively forced harmonic oscillator with friction. When the 'natural' frequency of the 'oscillator', $(G_0 + 2\Gamma_0(1 + c_{jl}))(2(1 + c_{jl}))^{1/2}$, equals the driving frequency, resonance occurs. This condition reads

$$[G_0 + 2\Gamma_0(1 + c_{jl})](2(1 + c_{jl}))^{1/2} = 4. \qquad (3.17)$$

Owing to the non-zero damping coefficient, $2\gamma(2(1 + c_{jl}))^{1/2}$, this resonance results in a finite value for $H_{jl}$ that is inversely proportional to the damping coefficient. We note that the parametric forcing term $h_2\sin 2t$ in (3.14) is not directly relevant to the resonant interaction.

The values of $\theta_{jl}$ ($c_{jl} = \cos\theta_{jl}$) that satisfy the resonance condition (3.17) as a function of $\Gamma_0$ are shown in figure 1(*a*). Since the right-hand side of (3.16) is proportional to $A_jA_l$, there are three waves involved in this resonance, namely standing wave modes $A_j$ and $A_l$, and mode $B$ with wavevector $\hat{k}_j + \hat{k}_l$, as shown in figure 1(*b*). Therefore, (3.16) describes a three-wave resonant interaction. Note that the wavenumber for mode $B$ is away from the critical wavenumber $k_0 = 1$, and thus mode $B$ is a linearly stable mode. For $\Gamma_0 < 1/3$, triad resonance is not possible. For $\Gamma_0 = 1/3$, wavevectors of the three resonating waves are in the same direction ($\theta_{jl}^{(r)} = 0$). As $\Gamma_0$ is further increased, $\theta_{jl}^{(r)}$ also increases. For purely capillary waves ($\Gamma_0 = 1$), $\theta_{jl}^{(r)}$ reaches the maximum value of $c_{jl} = 2^{1/3} - 1$ or $\theta_{jl}^{(r)} \approx 74.9°$.

Resonant interactions among surface capillary–gravity waves in general have been studied since the pioneering work by Wilton (1915) (for a recent review see Hammack & Henderson 1993). Wilton found that a Stokes expansion in powers of the wave amplitude became singular at a wavenumber $k = (g_0\rho/2\Gamma)^{1/2}$ for inviscid capillary–gravity waves in two spatial dimensions, which corresponds to the triad resonance discussed above for $\Gamma_0 = 1/3$.

This special case of resonant interaction is often termed *second-harmonic resonance* and the corresponding capillary–gravity waves are called Wilton's ripples.

Experimental studies by McGoldrick (1970), and Banerjee & Korpel (1982) on triad resonance in capillary–gravity waves have verified the function $\theta_{jl}^{(r)}$ (see figure 1a) quantitatively.†

The relevance of triad resonant interactions at second order to pattern formation in Faraday waves has been largely overlooked by previous studies. We want to emphasize here that the effect of triad resonant interactions on pattern formation in parametric surface waves can be intuitively understood. Let us consider a situation in which two linearly unstable standing waves $A_j$ and $A_l$ with their wavevectors separated by exactly the resonating angle $\theta_{jl}^{(r)}$ grow from small amplitudes in the linear regime. When they enter the nonlinear regime, a mode $B$ with wavevector $\hat{\boldsymbol{k}}_j + \hat{\boldsymbol{k}}_l$ is created as a result of quadratic nonlinear interaction of $A_j$ and $A_l$. The amplitude of $B$ will become very large because of the resonance and weak damping. For inviscid fluids, the amplitude of $B$ will increase without limit. Since the parametric forcing pumps energy into the surface wave system through unstable modes $A_j$ and $A_l$ at a rate determined by the supercriticality $\varepsilon$, the energy required for the growth of mode $B$ will come from reductions of the amplitudes in $A_j$ and $A_l$, but not directly from the external parametric force. As a result, the modes $A_j$ and $A_l$ will have smaller amplitudes than other unstable modes that do not satisfy the triad resonance condition. In other words, small perturbations with components close to the critical wavenumber will grow exponentially. When the amplitudes of these modes become large enough, a nonlinear selection process takes place such that modes with their wavevectors separated by the resonating angle $\theta_{jl}^{(r)}$ are less favoured or avoided. The above argument is relevant for both inviscid and weakly viscous fluids. For fluids of high viscosity, the influence of triad resonant interactions becomes smaller because of the large damping.

Since there is no solvability condition at second order, there will be no quadratic terms in the amplitude equations to be derived. Thus, the above described influence of triad resonant interactions must appear through cubic nonlinear terms, which represent four-wave resonant interactions among four linearly unstable standing wave modes. Specifically, in particular the coefficient of the cubic nonlinear terms in the amplitude equations is expected to have a large positive peak at the resonating angle $\theta_{jl}^{(r)}$ as we show later in this section. When viscous damping effects are neglected, the peak shifts toward $+\infty$. Such divergence of the nonlinear interaction coefficient was encountered by Milner (1991) in his analysis of weakly damped parametric surface waves because he neglected the contribution to the amplitude equation from the second-order solution. As a consequence, he failed to realize the relevance of such a divergence to pattern selection. In contrast, and in agreement with our calculations, Edwards & Fauve (1994) have suggested recently that triad resonance could be important for pattern selection.

As we show later, the occurrence of a standing wave pattern of square symmetry in capillary Faraday waves is closely related to triad resonance with $\theta_{jl}^{(r)} = 74.9°$. By increasing the gravity wave component in capillary–gravity waves, the resonating angle $\theta_{jl}^{(r)}$ becomes smaller and the nonlinear interaction coefficients at cubic order change accordingly. For $\Gamma_0 \approx 1/3$, $\theta_{jl}^{(r)}$ is close to zero and we will show that standing wave patterns of square symmetry become unstable and hexagonal, triangular, or quasi-crystalline patterns can be stabilized.

† Banerjee & Korpel (1982) measured the function $\theta_{jl}^{(r)}$ by exciting two plane waves with wavevector differing by a specified angle, and measuring the amplitude of the resulting wave. Hogan (1984) later resolved some discrepancy between the experimental measurements and theoretical predictions.

The solution of the corresponding homogeneous equation of (3.14) will have the same form as the solution at $O(\varepsilon^{1/2})$, and thus can be absorbed into the solution at $O(\varepsilon^{1/2})$. As a result, we are only interested in the particular solutions to the inhomogeneous equation for $h_2$. The particular solutions are

$$h_2 = \sum_{j,l=1}^{N} \Big\{ \left(\alpha_{jl} + \beta_{jl}\cos 2t + \gamma\delta_{jl}\sin 2t\right) \left[A_j A_l \exp\left(\mathrm{i}(\hat{\boldsymbol{k}}_j + \hat{\boldsymbol{k}}_l)\cdot\boldsymbol{x}\right) + \mathrm{c.c.}\right]$$
$$+ \left(\bar{\alpha}_{jl} + \bar{\beta}_{jl}\cos 2t + \gamma\bar{\delta}_{jl}\sin 2t\right) \left[A_j A_l^* \exp\left(\mathrm{i}(\hat{\boldsymbol{k}}_j - \hat{\boldsymbol{k}}_l)\cdot\boldsymbol{x}\right) + \mathrm{c.c.}\right]\Big\}, \quad (3.18)$$

where

$$\alpha_{jl} = \frac{1 + c_{jl}}{4\left[G_0 + 2\Gamma_0(1 + c_{jl})\right]} - \frac{2\gamma^2\delta_{jl}}{G_0 + 2\Gamma_0(1 + c_{jl})}, \quad (3.19)$$

$$\beta_{jl} = \frac{-\left(1 + c_{jl} - \frac{1}{4}(3 - c_{jl})(2(1 + c_{jl}))^{1/2}\right)\left(D_{jl} - 8\gamma^2 M_{jl}\right) + 8\gamma^2(1 + c_{jl})N_{jl}}{64\gamma^2(1 + c_{jl})^2 + D_{jl}^2 - 8\gamma^2 D_{jl}M_{jl}}, \quad (3.20)$$

$$\delta_{jl} = -\frac{8(1 + c_{jl})\left(1 + c_{jl} - \frac{1}{4}(3 - c_{jl})(2(1 + c_{jl}))^{1/2}\right) + D_{jl}N_{jl}}{64\gamma^2(1 + c_{jl})^2 + D_{jl}^2 - 8\gamma^2 D_{jl}M_{jl}}, \quad (3.21)$$

and

$$M_{jl} = \frac{(2(1 + c_{jl}))^{1/2}}{G_0 + 2\Gamma_0(1 + c_{jl})}, \quad (3.22)$$

$$D_{jl} = \left[G_0 + 2\Gamma_0(1 + c_{jl})\right](2(1 + c_{jl}))^{1/2} - 4, \quad (3.23)$$

$$N_{jl} = \left(\tfrac{5}{2} + c_{jl}\right)\left(1 + c_{jl} - (2(1 + c_{jl}))^{1/2}\right) + \tfrac{1}{8}(1 + c_{jl})(2(1 + c_{jl}))^{1/2} + (1 + c_{jl})M_{jl}. \quad (3.24)$$

$\bar{\alpha}_{jl}$, $\bar{\beta}_{jl}$, and $\bar{\delta}_{jl}$ can be obtained by replacing $c_{jl}$ with $-c_{jl}$ in the expressions for $\alpha_{jl}$, $\beta_{jl}$, and $\delta_{jl}$ respectively. The triad resonance occurs when $D_{jl} = 0$. We have retained terms that are proportional to $\gamma^2$ in the expressions for $\alpha_{jl}$, $\beta_{jl}$, and $\delta_{jl}$ since these terms become important when $D_{jl}$ is small or zero, i.e. at triad resonance. The factor $\gamma^2$ in these terms will either cancel to give terms of $O(1)$, or partially cancel to give terms of $O(1/\gamma)$. Although we still keep them when away from resonance, these terms are very small for weak damping, and thus should not affect the consistency of the perturbation expansion.

From (3.13), we have

$$\hat{\mathscr{D}}\Phi_2 = \partial_t h_2 - \gamma\nabla^2 h_2 + \nabla\cdot(h_1\nabla\Phi_1) + \hat{\mathscr{D}}\left(h_1\hat{\mathscr{D}}\Phi_1\right). \quad (3.25)$$

On substituting the expressions for $h_1$, $\Phi_1$, and $h_2$ into the above equation, we obtain the following expression for $\Phi_2$:

$$\Phi_2 = \sum_{j,l=1}^{N} \Big\{ \left(\gamma u_{jl} + \gamma v_{jl}\cos 2t + w_{jl}\sin 2t\right) \left[A_j A_l \exp\left(\mathrm{i}(\hat{\boldsymbol{k}}_j + \hat{\boldsymbol{k}}_l)\cdot\boldsymbol{x}\right) + \mathrm{c.c.}\right]$$
$$+ \left(\gamma\bar{u}_{jl} + \gamma\bar{v}_{jl}\cos 2t + \bar{w}_{jl}\sin 2t\right) \left[A_j A_l^* \exp\left(\mathrm{i}(\hat{\boldsymbol{k}}_j - \hat{\boldsymbol{k}}_l)\cdot\boldsymbol{x}\right) + \mathrm{c.c.}\right]\Big\}, \quad (3.26)$$

where

$$u_{jl} = \tfrac{1}{2} + \left(\alpha_{jl} - \tfrac{1}{4}\right)(2(1 + c_{jl}))^{1/2}, \quad (3.27)$$

$$v_{jl} = \tfrac{3}{4} + \left(\beta_{jl} - \tfrac{3}{8}\right)(2(1 + c_{jl}))^{1/2} + \frac{2\delta_{jl}}{(2(1 + c_{jl}))^{1/2}}, \tag{3.28}$$

$$w_{jl} = -\tfrac{1}{2} + \tfrac{1}{4}(2(1 + c_{jl}))^{1/2} - \frac{2\beta_{jl}}{(2(1 + c_{jl}))^{1/2}}, \tag{3.29}$$

and $\bar{u}_{jl}$, $\bar{v}_{jl}$, and $\bar{w}_{jl}$ can be obtained by replacing $c_{jl}$ with $-c_{jl}$ in the expressions for $u_{jl}$, $v_{jl}$, and $w_{jl}$ respectively. We also note that $v_{jl}$ and $w_{jl}$ are not singular at $c_{jl} = -1$ since the factor in denominator $(2(1 + c_{jl}))^{1/2}$ will be cancelled by the same factor in the numerator in (3.28) and (3.29). Similarly, $\bar{v}_{jl}$ and $\bar{w}_{jl}$ are also not singular at $c_{jl} = 1$.

The amplitude $A_j$ are not determined yet at $O(\varepsilon)$, and thus it is necessary to continue the expansion to higher orders. At $O(\varepsilon^{3/2})$, we have

$$\mathscr{L}\begin{pmatrix} h_3 \\ \Phi_3 \end{pmatrix} = \begin{pmatrix} -\partial_T h_1 - \nabla \cdot (h_1 \nabla \Phi_2 + h_2 \nabla \Phi_1) - \hat{\mathscr{D}}\left(h_1 \hat{\mathscr{D}} \Phi_2 + h_2 \hat{\mathscr{D}} \Phi_1\right) \\ -\partial_T \Phi_1 - 4\gamma h_1 \sin 2t + \hat{\mathscr{D}} \Phi_1 \hat{\mathscr{D}} \Phi_2 - \nabla \Phi_1 \cdot \nabla \Phi_2 \end{pmatrix}$$

$$+ \begin{pmatrix} \hat{\mathscr{D}}\left[h_1 \hat{\mathscr{D}}(h_1 \hat{\mathscr{D}} \Phi_1) + \tfrac{1}{2} h_1^2 \nabla^2 \Phi_1\right] + \tfrac{1}{2} \nabla^2 \left(h_1^2 \hat{\mathscr{D}} \Phi_1\right) \\ -\hat{\mathscr{D}} \Phi_1 \left[h_1 \nabla^2 \Phi_1 + \hat{\mathscr{D}}(h_1 \hat{\mathscr{D}} \Phi_1)\right] - \tfrac{1}{2}\Gamma_0 \nabla \cdot \left(\nabla h_1 (\nabla h_1^2)\right) \end{pmatrix}. \tag{3.30}$$

We have found that it is convenient to obtain the solvability condition at this order from the independent equation for $h_3$, which can be easily obtained from (3.30), and it reads

$$\partial_{tt} h_3 - 2\gamma \nabla^2 \partial_t h_3 + (G_0 - \Gamma_0 \nabla^2)\hat{\mathscr{D}} h_3 + 4\gamma \sin 2t \hat{\mathscr{D}} h_3 = -\partial_T ((\gamma + \partial_t) h_1 + \Phi_1)$$

$$- 4\gamma h_1 \sin 2t + \left(\gamma \nabla^2 - \partial_t\right)\left[\nabla \cdot (h_1 \nabla \Phi_2 + h_2 \nabla \Phi_1) + \hat{\mathscr{D}}\left(h_1 \hat{\mathscr{D}} \Phi_2 + h_2 \Phi_1\right)\right.$$

$$+ \hat{\mathscr{D}}\left(\tfrac{1}{2} h_1^2 \Phi_1 - h_1 \hat{\mathscr{D}}(h_1 \Phi_1)\right) - \tfrac{1}{2} \nabla^2 \left(h_1^2 \Phi_1\right)\right]$$

$$+ \hat{\mathscr{D}}\left[\Phi_1 \hat{\mathscr{D}} \Phi_2 - \nabla \Phi_1 \cdot \nabla \Phi_2 + \Phi_1^2 h_1 - \Phi_1 \hat{\mathscr{D}}(h_1 \Phi_1) - \tfrac{1}{2}\Gamma_0 \nabla \cdot \left(\nabla h_1 (\nabla h_1)^2\right)\right]. \tag{3.31}$$

The Fredholm alternative theorem requires that the right-hand side of (3.31) be orthogonal to any of the independent solutions of its adjoint homogeneous equation. The solvability condition reads

$$\int_0^{2\pi} \mathrm{d}t \int_0^{2\pi} \mathrm{d}\Theta_j \mathrm{RHS}_3 \tilde{h}_j(\boldsymbol{x}, t) = 0, \tag{3.32}$$

where $\mathrm{RHS}_3$ stands for the right-hand side of (3.31), and $\tilde{h}_j(\boldsymbol{x}, t)$ is either one of the following two independent solutions of the adjoint homogeneous equation:

$$\left(\cos t + \tfrac{1}{4}\gamma \sin 3t + \ldots\right) \exp\left(\pm \mathrm{i}\hat{\boldsymbol{k}}_j \cdot \boldsymbol{x}\right),$$

$$\left(\sin t - \tfrac{1}{4}\gamma \cos 3t + \ldots\right) \exp\left(\pm \mathrm{i}\hat{\boldsymbol{k}}_j \cdot \boldsymbol{x}\right),$$

where $\hat{\boldsymbol{k}}_j$ is a unit vector in an arbitrary direction, and $\Theta_j = \hat{\boldsymbol{k}}_j \cdot \boldsymbol{x}$. Since both $\mathrm{RHS}_3$ and $\tilde{h}_j(\boldsymbol{x}, t)$ have a temporal period $2\pi$, we have taken the interval of integration in (3.32) to be $2\pi$. Also because of the periodicity of $\mathrm{RHS}_3$ and $\tilde{h}_j(\boldsymbol{x}, t)$, it is only necessary to consider the term proportional to $\cos t$ or $\sin t$ in $\tilde{h}_j(\boldsymbol{x}, t)$. It turns

out that the relevant solvability condition is obtained from the second solution of $\tilde{h}_j(x, t)$. If we had also considered the linearly stable mode $B_j$ in this analysis, another solvability condition would be obtained from the first solution of $\tilde{h}(t)$. In summary, the solvability condition for (3.31) is that the coefficient of $\sin t \exp(\pm i\hat{k}_j \cdot x)$ term in RHS₃ equals zero.

In what follows, we will collect terms from the right-hand side of (3.31) that are relevant to the solvability condition in a tedious but straightforward calculation. These terms can be written as

$$
\text{RHS} = 2\sin t \sum_{j=1}^{N} \left\{ \left[ \partial_T A_j - \gamma A_j + \gamma \left( \left( \frac{28 + 9\Gamma_0}{64} + 2\alpha_{jj} + \tfrac{3}{8}\beta_{jj} - \tfrac{1}{2}\delta_{jj} \right) |A_j|^2 \right. \right. \right.
$$
$$
\left. \left. \left. + \sum_{l=1(l\neq j)}^{N} g(c_{jl})|A_l|^2 \right) A_j \right] \exp\left( i\hat{k}_j \cdot x \right) + \text{c.c.} \right\} + \dots,
$$

where

$$
g(c_{jl}) = \frac{3\Gamma_0}{32} \left( 1 + 2c_{jl}^2 \right) + \tfrac{7}{8} \left( 3 - (2(1 + c_{jl}))^{1/2} - (2(1 - c_{jl}))^{1/2} \right)
$$
$$
+ \left( 1 + c_{jl} - (2(1 + c_{jl}))^{1/2} \right) \left( \tfrac{1}{4}w_{jl} - v_{jl} \right)
$$
$$
+ \left( 1 - c_{jl} - (2(1 - c_{jl}))^{1/2} \right) \left( \tfrac{1}{4}\bar{w}_{jl} - \bar{v}_{jl} \right)
$$
$$
+ (1 + c_{jl}) \left( 2\alpha_{jl} + \tfrac{3}{8}\beta_{jl} - \tfrac{1}{2}\delta_{jl} \right) + (1 - c_{jl}) \left( 2\bar{\alpha}_{jl} + \tfrac{3}{8}\bar{\beta}_{jl} - \tfrac{1}{2}\bar{\delta}_{jl} \right). \quad (3.33)
$$

The solvability condition therefore reads

$$
\frac{\partial A_j}{\partial T} = \gamma A_j - \left[ \gamma g(1)|A_j|^2 + \gamma \sum_{l=1(l\neq j)}^{N} g(c_{jl})|A_l|^2 \right] A_j, \quad (3.34)
$$

where $j = 1, 2, \cdot s, N$ and

$$
g(1) = \frac{28 + 9\Gamma_0}{64} + 2\alpha_{jj} + \tfrac{3}{8}\beta_{jj} - \tfrac{1}{2}\delta_{jj}. \quad (3.35)
$$

Equation (3.34) is the coupled set of standing wave amplitude equations (SWAE) for $A_j$, which is the central result of this weakly nonlinear analysis. The generic form of the above set of amplitude equations is of course quite general and has been derived for a number of different physical systems (Cross & Hohenberg 1993; Newell, Passot & Lega 1993). The behaviour peculiar to each system stems from the functional form of the nonlinear interaction coefficients $g(1)$ and $g(c_{jl})$, and from the time constant $\tau_0$ ($\tau_0 = 1/\gamma$, in the case of Faraday waves).

Before we look at the quantitative details of the nonlinear coefficients, $g(1)$ and $g(c_{jl})$, we make the following comments on the SWAEs.

(i) The exclusion of quadratic nonlinear terms in the SWAEs, which is related to the absence of solvability conditions at $O(\varepsilon)$, is a consequence of the requirement of sign invariance of the SWAEs ($A_j \rightarrow -A_j$). Subharmonic response of the fluid surface to the driving force $f\sin(2\omega_0 t)$ implies $h(x, t + \pi/\omega_0) = -h(x, t)$, where $h$ is a linear unstable mode given by (3.6). We note that a sign change of the amplitude $A_j$ is equivalent to a time displacement in a period of the driving force, $t \rightarrow t + \pi/\omega_0$. Because of the invariance of the original fluid equations under such a time displacement, the amplitude equation of $A_j$ must be invariant under a sign change in $A_j$.

(ii) The coefficients of cubic nonlinear terms, $\gamma g(1)$ and $\gamma g(c_{jl})$, are proportional to the linear damping coefficient $\gamma$. This result is qualitatively different from that obtained by Milner (1991). He also derived a coupled set of standing wave amplitude equations of the same form as (3.34). Although his nonlinear coefficients are also proportional to $\gamma$ (the dissipation function $Q$ is after all proportional to the kinematic viscosity $v$), they result entirely from nonlinear viscous terms in the dissipation function. In fact, linear viscous terms did not contribute at all to third order. The appearance of nonlinear terms proportional to the linear damping coefficient $\gamma$ in the SWAEs in our approach is, however, no surprise. In general, a parameter that appears in the coefficients of the linear terms in the original equations can appear in the coefficients of nonlinear terms of the amplitude equations for that system. For example, the nonlinear interaction coefficient in the amplitude equation for Rayleigh–Bénard convection is a function of the Prandtl number $Pr$, although $Pr$ appears only in the coefficients for linear terms in the Boussinesq equations (see e.g. Cross 1980). Throughout this paper, nonlinear terms that are proportional to the kinematic viscosity $v$ in the fluid equations (or the QPEs, (2.9)–(2.13)) are termed *nonlinear viscous terms*, and the nonlinear terms proportional to $v$ or $\gamma$ in amplitude equations for Faraday waves are termed *nonlinear damping terms* in order to avoid confusion due to terminology. The validity of the quasi-potential equations with only linear viscous terms relies on the assumption that nonlinear viscous terms do not have a significant effect on pattern formation in Faraday waves. A check of the validity can only be provided by comparing our results to experimental studies.

(iii) There are contributions to the nonlinear terms of (3.34) from the parametric driving force. These contributions are proportional to the driving amplitude $f$, but they appear in (3.34) together with the contributions from the linear viscous terms in the QPEs since we have set $f = \gamma$ in the linear solutions ((3.11) and (3.12)). The contributions from the parametric driving force are directly related to the higher-harmonic terms proportional to $f$ in the linear solutions for $h$ and $\Phi$. This contribution provides the *amplitude-limiting effect* by the driving force, which results from the nonlinear interaction of these higher-harmonic terms with the primary mode, which has half the driving frequency. Such nonlinear interactions produces terms that are out of phase by $\pi/2$ with the primary mode, and thus possibly damp or limit the wave amplitude. An important point is that this amplitude-limiting effect results from non-dissipative terms in the governing equation and so is also important for inviscid systems. This effect by the driving force, to our knowledge, has not been identified before. A different amplitude-limiting effect also through non-dissipative terms was studied by Zakharov, Lvov & Starobinets (1975) in the context of parametric spin-wave systems. Zakharov *et al.* studied parametric spin-wave instabilities, and considered the deviation of the phase of the excited spin waves from the optimum phase as the major nonlinear mechanism which limits the parametric instability. However, we agree with Cross & Hohenberg (1993) that this 'de-phasing' effect of the parametric mode is small (of higher order) close to threshold.

Owing to the mode interference occurring exactly at $c_{jl} = 1$ ($j = l$ or $\theta_{jl} = 0$), $g(c_{jl})$ is not a smooth function of $c_{jl}$. It is easy to show that

$$g(1) = \tfrac{1}{2}g(c_{jl} \to 1). \tag{3.36}$$

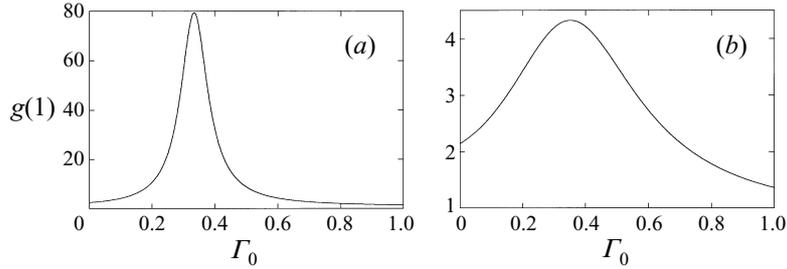We also note that

$$g(c_{jl}) = g(-c_{jl}). \tag{3.37}$$

FIGURE 2. The self-interaction coefficient $g(1)$ of the standing wave amplitude equations as a function of $\Gamma_0$ with the linear damping coefficient $\gamma = 0.1$ in (a), and $\gamma = 0.02$ in (b).

This symmetry is an obvious requirement for SWAEs since it is equivalent to have two standing waves separated by angle $\theta$ or by $\pi - \theta$.

An additional issue concerns the transformation of the equations of motion under time reversal, and the related question of the existence of cubic terms in (3.34) in the limit of a Hamiltonian system (i.e. in the absence of dissipative contributions to the equations of motion). Under time reversal, the variables of interest transform according to $t \to -t$, $\hat{\boldsymbol{k}}_j \to -\hat{\boldsymbol{k}}_j$ and $A_j(t) \to A_j^*(-t)$. We also note that the Hamiltonian equation (2.27) depends explicitly on time, and that given our choice of driving force proportional to $\sin 2t$, the trajectory of the system under time reversal is invariant only if, in addition to the transformation rules given above, $f \to -f$. A similar situation arises in systems with applied magnetic fields, or for Coriolis forces, in which either the magnetic field or the angular velocity must be reversed. In the absence of viscous dissipation ($\gamma = 0$), the only nonlinear terms in the SWAEs come from the driving force, and are proportional to the driving amplitude $f$. These terms can be written as

$$-f \left[ g(1)|A_j|^2 + \sum_{l=1(l \neq j)}^{N} g(c_{jl})|A_l|^2 \right] A_j.$$

Thus, nonlinear terms proportional to $f$ do change sign under time reversal, and are allowed in the equations of motion for the amplitudes $A_j$. This conclusion is not trivially related to having chosen a sine function as the driving force. Had we chosen $f \cos(2t)$ as the forcing term, the linearly growing modes would be a combination of $A_j$ and $B_j$, but while the algebra for the derivation of the SWAEs becomes more tedious the final conclusion remains the same even though, in this latter case, $f$ would be formally chosen to be invariant under time reversal. On the other hand, for an autonomous system in which the Hamiltonian does not explicitly depends on time, if the cubic term in (3.34) is entirely of Hamiltonian character, then invariance under time reversal implies $\sum_l g(c_{jl})|A_l|^2 A_j = 0$, for any arbitrary set of amplitudes. This equality is satisfied if $g(c_{jl}) = -g(-c_{jl})$, where $c_{jl}$ involves the interaction between modes $\hat{\boldsymbol{k}}_j$ and $\hat{\boldsymbol{k}}_l$, and $-c_{jl}$ between $\hat{\boldsymbol{k}}_j$ and $-\hat{\boldsymbol{k}}_l$ (see figure 1 and Cross & Hohenberg 1993). This symmetry together with (3.37) would imply that $g(c_{jl}) = 0$ in this case. Therefore, saturation of the wave amplitude would have to occur either through weak nonlinear dissipative effects, or higher-order terms (e.g. nonlinear frequency detuning terms).

Figure 2 shows the self-interaction coefficient $g(1)$ as a function of $\Gamma_0$ for two different values of $\gamma = 0.1$ and $0.02$. The maxima in the curves around $\Gamma_0 = 1/3$ are
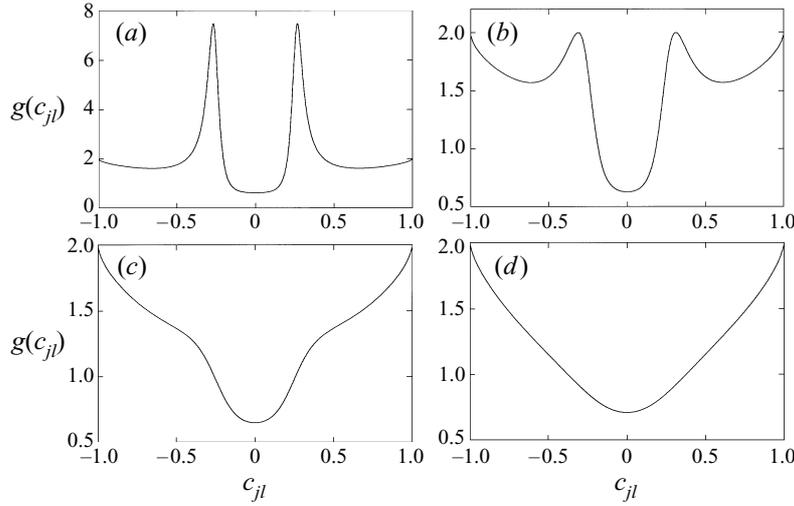
FIGURE 3. The standing wave nonlinear coefficient $g(c_{jl})$ as a function of $c_{jl}$ for purely capillary waves ($\Gamma_0 = 1$) with the linear damping coefficient $\gamma = 0.02$ in ($a$), $\gamma = 0.05$ in ($b$), $\gamma = 0.1$ in ($c$), and $\gamma = 0.2$ in ($d$).

the result of the triad resonant interaction of standing waves in the same direction, namely $\theta_{jl}^{(r)} = 0$ (the second-harmonic resonance), that affect $g(1)$. Since the resonance is less damped for smaller values of $\gamma$, the value of the coefficient $g(1)$ varies inversely with damping.

Since $g(1) > 0$, we can rescale the amplitude as $\tilde{A}_j = (g(1)A_j)^{1/2}$. We have the following SWAE for the scaled amplitude:

$$\frac{1}{\gamma}\frac{\partial \tilde{A}_j}{\partial T} = \tilde{A}_j - \left[ |\tilde{A}_j|^2 + \sum_{l=1(l \neq j)}^{N} \tilde{g}(c_{jl})|\tilde{A}_l|^2 \right] \tilde{A}_j, \tag{3.38}$$

where $\tilde{g}(c_{jl}) = g(c_{jl})/g(1)$. From (3.36) and symmetry for $\pm c_{jl}$, we also have $\tilde{g}(c_{jl} \to \pm 1) = 2$.

The nonlinear interaction coefficient $g(c_{jl})$ in (3.38) (we have suppressed the tilde since we will only refer to the scaled nonlinear coefficient in what follows) depends on the dimensionless fluid parameters $\Gamma_0$ (or $G_0$) and $\gamma$. Figure 3 shows the function $g(c_{jl})$ for four different values of the damping coefficient $\gamma$. The maxima in $g(c_{jl})$ around $c_{jl} = 0.26$ ($\theta_{jl} = 74.9°$) correspond to triad resonance for purely capillary waves (see figure 1). Even for relatively large values of the damping coefficient $\gamma = 0.2$, the influence of the triad resonance on the $g(c_{jl})$ curve can still be seen, but becomes much weaker. An important feature common to all the curves in figure 3 is that there is a minimum of $g(c_{jl})$ at $c_{jl} = 0$, and $g(0) < 1$. It is also interesting to compare the differences in $g(c_{jl})$ for purely capillary waves ($\Gamma_0 = 1$), purely gravity waves ($\Gamma_0 = 0$), and mixed gravity–capillary waves ($0 < \Gamma_0 < 1$) since the triad resonant interaction strongly depends on the value of $\Gamma_0$. Figure 4 shows the function $g(c_{jl})$ for four different values of damping coefficients (the same as in figure 3) for purely gravity waves ($\Gamma_0 = 0$). We note that because of the absence of triad resonant interaction, the variations among the $g(c_{jl})$ curves for different values of $\gamma$ are quite small. The curves still have minima at $c_{jl} = 0$, but the minima are much flatter.

Since the triad resonant interaction occurs among waves with their wave vectors in the same direction when $\Gamma_0 = 1/3$, finally we examine the function $g(c_{jl})$
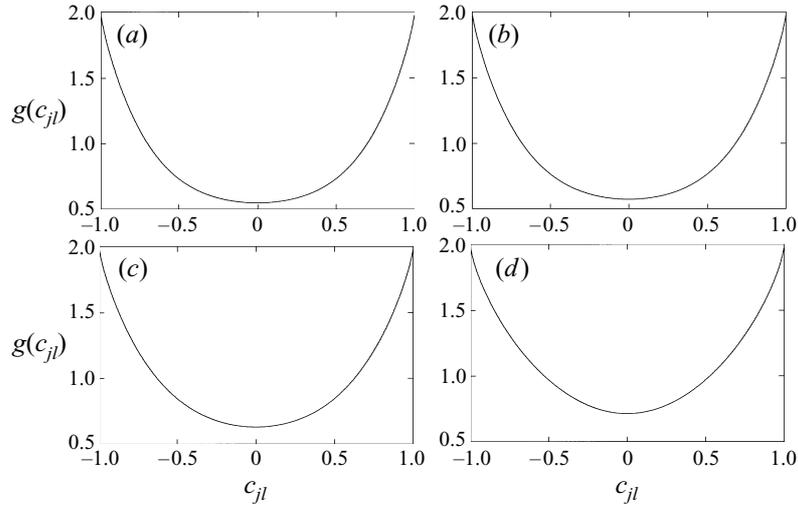
FIGURE 4. The nonlinear coefficient $g(c_{jl})$ of the standing wave amplitude equation as a function of $c_{jl}$ for purely gravity waves ($\Gamma_0 = 0$) with the linear damping coefficient $\gamma = 0.02$ in (a), $\gamma = 0.05$ in (b), $\gamma = 0.1$ in (c), and $\gamma = 0.2$ in (d).

for this case. Figure 5 shows $g(c_{jl})$ for four different values of the damping coefficient (the same as in figure 3) for capillary–gravity waves with $\Gamma_0 = 1/3$. We observe that $g(c_{jl})$ is very flat and reaches very small positive values for small values of $\gamma$. These facts are a consequence of the second-harmonic resonance, since the value of $g(1)$ becomes very large (see figure 2) for this special case of triad resonant interaction. For relatively large values of the damping parameter, e.g. $\gamma = 0.20$, the effect of the second-harmonic resonance is much smaller.

### 3.3. *Pattern selection near onset*

Equation (3.38) is of gradient form $(1/\gamma)\partial_T A_j = -\partial \mathscr{F}/\partial A_j^*$, with Lyapunov function $\mathscr{F}$ given by

$$\mathscr{F} = -\sum_{j=1}^{N} |A_j|^2 + \frac{1}{2}\sum_{j=1}^{N} |A_j|^2 \left( |A_j|^2 + \sum_{l=1(l\neq j)}^{N} g(c_{jl})|A_l|^2 \right). \qquad (3.39)$$

Since

$$\frac{\mathrm{d}\mathscr{F}}{\mathrm{d}T} = \sum_{j=1}^{N} \left( \frac{\partial \mathscr{F}}{\partial A_j}\partial_T A_j + \frac{\partial \mathscr{F}}{\partial A_j^*}\partial_T A_j^* \right) = -\frac{2}{\gamma}\sum_{j=1}^{N} |\partial_T A_j|^2 \leqslant 0, \qquad (3.40)$$

the only possible limiting cases of such a dissipative system, in the limit $T \to \infty$, are stationary states for the amplitudes $A_j$. Only the states which correspond to local minima of the Lyapunov function are linearly stable.

Apart from the trivial solution of $A_j = 0$ for $j = 1, \ldots, N$, (3.38) has a family of stationary solutions differing in the total number of standing waves $N$ for which $A_j \neq 0$. By considering the case in which the magnitudes of all standing waves are
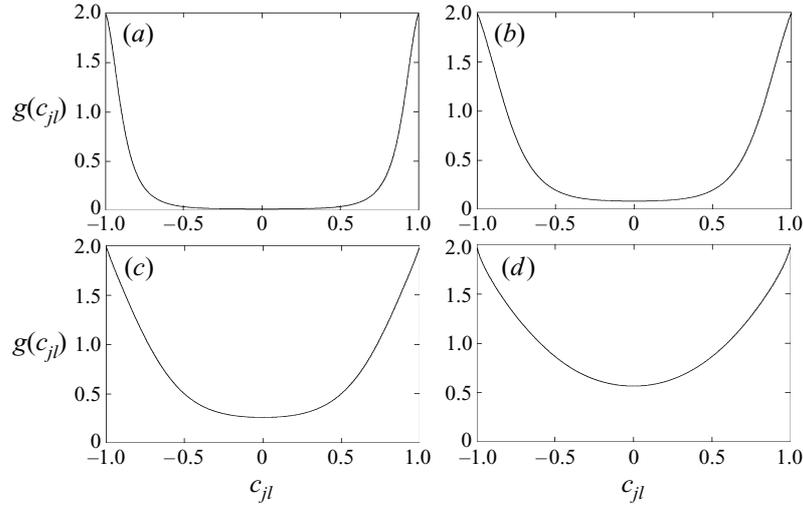
FIGURE 5. The nonlinear coefficient $g(c_{jl})$ of the standing wave amplitude equation as a function of $c_{jl}$ for gravity–capillary waves of $\Gamma_0 = 1/3$ with the linear damping coefficient $\gamma = 0.02$ in (a), $\gamma = 0.05$ in (b), $\gamma = 0.1$ in (c), and $\gamma = 0.2$ in (d).

the same, i.e. $|A_j| = |A|$, (3.38) has the following solutions:

$$|A_j| = |A| = \left( 1 + \sum_{l=1(l\neq j)}^{N} g(c_{jl}) \right)^{-1/2}. \tag{3.41}$$

The values of the Lyapunov function for these solutions are,

$$\mathscr{F} = -\tfrac{1}{2} N |A|^2 = -\frac{\tfrac{1}{2} N}{1 + \displaystyle\sum_{l=1(l\neq j)}^{N} g(c_{jl})}. \tag{3.42}$$

We note that the greater the square of the amplitude, the lower value of the Lyapunov function. Also the larger the values of $g(c_{jl})$ for a standing wave pattern, the larger value of the Lyapunov function. In particular, if an angle separating the wavevectors of two standing wave modes of the pattern satisfies the triad resonant condition, the corresponding $g(c_{jl})$, and thus the value of the Lyapunov function, will be large. Therefore, such patterns are not likely to appear. This result is consistent with our intuitive understanding of the role of the triad resonant interaction, i.e. the system tries to avoid pairs of standing waves with their wavevectors separated by an angle satisfying the triad resonant condition.

For $N = 1$ (parallel roll solution), $\mathscr{F}_1 = -\frac{1}{2}$. For $N = 2$, we have either square ($c_{12} = 0$) or rhombic ($c_{12} \neq 0$) patterns with $\mathscr{F}_2 = -1/(1 + g(c_{12}))$. By considering regular patterns† only, for $N = 3$, we have either hexagonal or triangular patterns, which have the same value of the Lyapunov function

$$\mathscr{F}_3 = -\frac{\tfrac{3}{2}}{1 + g(\tfrac{1}{2}) + g(-\tfrac{1}{2})}.$$

† By regular patterns, we mean pattern structures for which the angle between any two adjacent wavevectors $\boldsymbol{k}_j$ and $\boldsymbol{k}_{j+1}$ is the same and amounts to $\pi/N$.
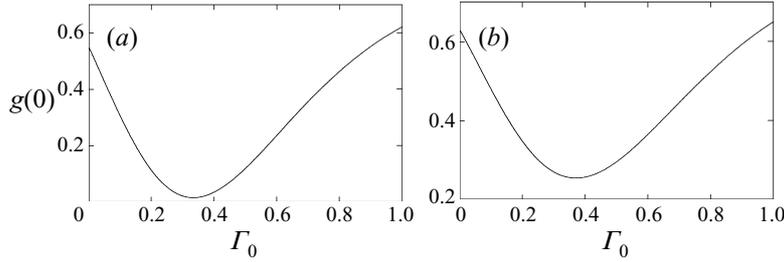
FIGURE 6. $g(0)$ as a function of $\Gamma_0$ for $\gamma = 0.1$ in (*a*) and $\gamma = 0.02$ in (*b*). The minima around $\Gamma_0 = 1/3$ are the consequence of the one-dimensional triad resonant interaction.
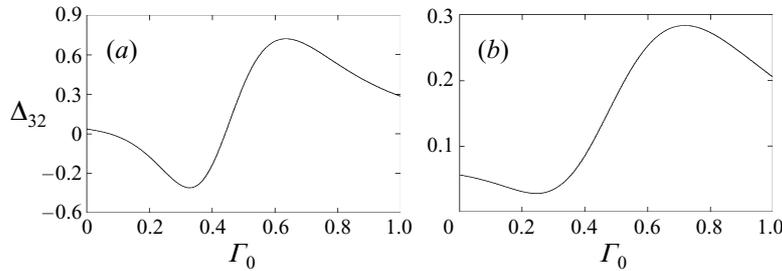


FIGURE 7. The difference $\Delta_{32}$ of the values of the Lyapunov function for hexagonal/triangular patterns $\mathscr{F}_3$ and square patterns $\mathscr{F}_2$ as a function of $\Gamma_0$ for $\gamma = 0.1$ in (*a*) and $\gamma = 0.02$ in (*b*).

We first consider square patterns for $N = 2$. If $g(0) < 1$, we have $\mathscr{F}_2 < \mathscr{F}_1 = -\frac{1}{2}$. As shown in figure 6 we indeed have $g(0) < 1$ for the interesting parameter range of $\Gamma_0$ and $\gamma$. Therefore standing wave patterns of square symmetry always have lower values of the Lyapunov function than parallel roll patterns for weakly damped parametric surface waves near onset.

In order to compare the values of the Lyapunov function for square patterns with that of hexagonal or triangular patterns, we compute the value of

$$\Delta_{32} \equiv \mathscr{F}_3 - \mathscr{F}_2 = \frac{1 + g(\frac{1}{2}) + g(-\frac{1}{2}) - \frac{3}{2}(1 + g(0))}{(1 + g(0))(1 + g(\frac{1}{2}) + g(-\frac{1}{2}))},$$

which is plotted in figure 7.

For $\gamma = 0.1$, we have $\Delta_{32} = \mathscr{F}_3 - \mathscr{F}_2 > 0$ for all values of $\Gamma_0$, and thus standing wave patterns of square symmetry also have lower values of the Lyapunov function than hexagonal/triangular patterns. We also note that the difference between $\mathscr{F}_3$ and $\mathscr{F}_2$ becomes smaller for smaller values of $\Gamma_0$. For $\gamma = 0.02$, we still have $\Delta_{32} = \mathscr{F}_3 - \mathscr{F}_2 > 0$ for capillary waves, but near the second-harmonic resonance ($\Gamma_0 = 1/3$), we have $\mathscr{F}_3 < \mathscr{F}_2$, i.e. hexagonal/triangular patterns have lower values of the Lyapunov function than square patterns.

Regular patterns for $N \geqslant 4$ are two-dimensional quasi-crystalline patterns (or quasi-patterns (Edwards & Fauve 1993, 1994)). A quasi-pattern has long-range orientational order but no spatial periodicity, and thus is analogous to a quasi-crystal in solid-state physics (Shechtman *et al.* 1984). For $N = 4$, the value of the Lyapunov function for an eightfold quasi-pattern is

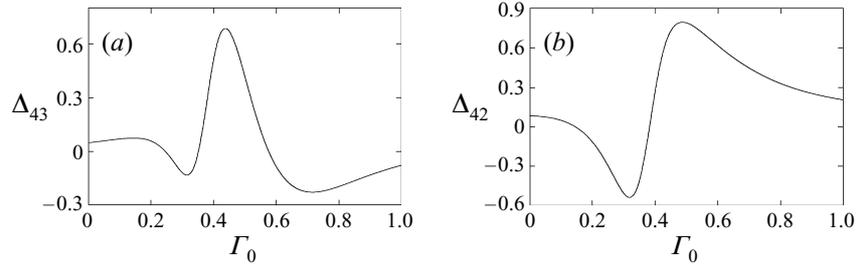$$\mathscr{F}_4 = -\frac{2}{1 + g(\frac{1}{2}\sqrt{2}) + g(0) + g(-\frac{1}{2}\sqrt{2})}.$$

FIGURE 8. The differences in the values of the Lyapunov function for eightfold quasi-patterns and hexagonal/triangular patterns, $\Delta_{43}$, in (*a*), and for eightfold quasi-patterns and square patterns, $\Delta_{42}$, in (*b*). In both cases, $\gamma = 0.02$.
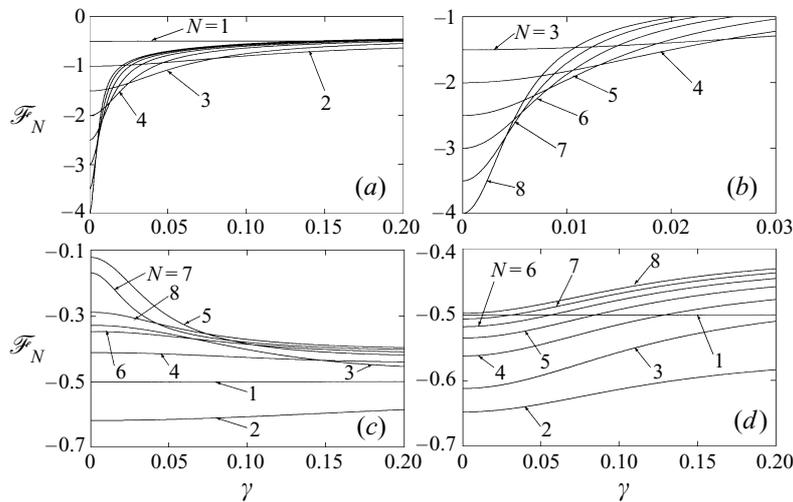


FIGURE 9. The values of the Lyapunov function $\mathscr{F}_N$ ($N = 1, 2, 3, 4, 5, 6, 7, 8$) as a function of $\gamma$ for $\Gamma_0 = 1/3$ in (*a*), $\Gamma_0 = 1$ (capillary waves) in (*c*), and $\Gamma_0 = 0$ (gravity waves) in (*d*). The portion of (*a*) with small values of $\gamma$ is shown in (*b*).

We are interested in any parameter range in which $\mathscr{F}_4$ has lower value of the Lyapunov function than $\mathscr{F}_2$ and $\mathscr{F}_3$. The most possible parameter range is certainly near the second-harmonic triad resonant interaction with very weak damping. We thus compute the values of

$$\Delta_{43} \equiv \mathscr{F}_4 - \mathscr{F}_3 = \frac{\frac{3}{2}(1 + g(0)) + 3g(\frac{1}{2}\sqrt{2}) - 2(1 + 2g(\frac{1}{2}))}{((1 + 2g(\frac{1}{2}))(1 + g(0) + 2g(\frac{1}{2}\sqrt{2}))},$$

and

$$\Delta_{42} \equiv \mathscr{F}_4 - \mathscr{F}_2 = \frac{2g(\frac{1}{2}\sqrt{2}) - (1 + g(0))}{(1 + g(0))(1 + g(0) + 2g(\frac{1}{2}\sqrt{2}))},$$

which are plotted in figure 8. We see indeed that for $\gamma = 0.02$ we have $\mathscr{F}_4 < \mathscr{F}_3$ and $\mathscr{F}_4 < \mathscr{F}_2$ around $\Gamma_0 = 1/3$.

We summarize our results concerning regular patterns in figure 9. We present the values of the Lyapunov function $\mathscr{F}_N$ as a function of $\gamma$ for $N = 1, 2, 3, 4, 5, 6, 7, 8$, and $\Gamma_0 = 1/3$, 1, and 0. For $\Gamma_0 = 1$ (figure 9*c*) and 0 ((figure 9*d*), patterns of square

| Range of $\gamma$ | Favoured pattern |
|---|---|
| $\gamma > 0.0809$ | square |
| $0.0253 < \gamma < 0.0809$ | hexagonal/triangular |
| $0.0132 < \gamma < 0.0253$ | eightfold quasi-patterns |
| $0.0082 < \gamma < 0.0132$ | tenfold quasi-patterns |
| $0.0057 < \gamma < 0.0082$ | twelvefold quasi-patterns |
| $0.0042 < \gamma < 0.0057$ | fourteenfold quasi-patterns |

TABLE 1. Patterns with the lowest values of the Lyapunov function and their corresponding ranges of $\gamma$. These values correspond to mixed capillary–gravity waves with $\Gamma_0 = 1/3$.

symmetry ($N = 2$) have the lowest values of $\mathscr{F}_N$ for all values of $\gamma < 0.2$, whereas the system favours patterns of different symmetries in different ranges of $\gamma$ for $\Gamma_0 = 1/3$. The second-harmonic resonance for $\Gamma_0 = 1/3$ becomes less damped as $\gamma$ decreases, and thus the value of the self-interaction nonlinear coefficient $g(0)$ becomes larger (see figure 6). In other words, the curve $g(c_{jl})$ has a wider flat centre region and a sharper increase near $c_{jl} = \pm 1$, and therefore pattern structures with larger $N$ are favoured. Table 1 shows the favoured structures, and the corresponding ranges of $\gamma$.

A couple of comments on the various patterns discussed above are in order. (i) A two-dimensional regular pattern structure with the spatial form $\sum_{j=1}^{N} \left( A_j \exp(i\hat{\boldsymbol{k}}_j \cdot \boldsymbol{x}) + \text{c.c.} \right)$ has $N$ degrees of freedom. These $N$ degrees of freedom appear as the phase of the complex amplitude $A_j = A_0 \exp(\theta_j)$ for $j = 1, \ldots, N$. Among them, two correspond to spatial translations, whereas the other $N - 2$ degrees of freedom represent the phason modes (Golubitsky, Swift & Knobloch 1984; Malomed, Nepomnyashchiĭ & Tribelskiĭ 1989). For $N = 3$, the phase degeneracy for the single phason mode, which corresponds to hexagonal or triangular states, can be lifted by higher-order nonlinear terms (Golubitsky *et al.* 1984; Müller 1993). Although it is beyond the scope of this article, it would be interesting to see how the phase relations of a spatial pattern are determined by higher-order nonlinear terms. (ii) We predict that quasi-patterns with large values of $N$ occur at very small values of the linear damping coefficient $\gamma$. As discussed in the introduction, for very small values of $\gamma$ the mode quantization effect can be quite severe for finite-size systems. This implies that experimental verification of the quasi-patterns with large values of $N$ can be difficult.† Obviously, a similar problem appears in numerical solutions of Faraday waves.

The linear stability of solutions (3.41) of the SWAEs (3.38) can be determined by the spectrum of growth rates $\sigma$ of amplitude perturbations $A_j \propto e^{\sigma t}$ since all phase perturbations are neutrally stable as is obvious from (3.38). Equivalently, the linear stability of solutions can also be obtained by the eigenvalue spectrum of the matrix $\partial^2 \mathscr{F}/(\partial|A_j|\partial|A_l|)$, linearized around the stationary solutions. In the context of the SWAEs (3.41), we can only consider a very limited set of perturbations. The usefulness of the stability analysis is to identify unstable solutions. A stable solution in the context of the SWAEs can, however, be unstable to other perturbations, such as a travelling wave mode or a perturbation with spatial variations. In the rest of

† In laboratory experiments, mode quantization also depends on the nature of boundary conditions. Certain 'soft' boundary conditions may relax the strict quantization requirements and allow access to the larger system regime than the actual size of the system (Douady 1990; Bechhoefer *et al.* 1995).

this subsection, stable or unstable solutions are with respect to the perturbations that are allowed by the SWAEs.

Let us consider a stationary solution with $|A_j| = a_0$ given by (3.41) for $j = 1, \ldots, N$ and $|A_j| = 0$ for $j = N + 1, \ldots, M$ ($M \geqslant N$), and small real perturbations $b_j$ to $|A_j|$ for $j = 1, \ldots, M$. On substituting the stationary solution with the perturbations into (3.38), we obtain the following linearized equations for $b_j$:

$$\frac{1}{\gamma} \partial_T b_j = \left[ 1 - a_0^2 \left( 3 + \sum_{l=1(l \neq j)}^{N} g(c_{jl}) \right) \right] b_j - 2a_0^2 \sum_{l=1(l \neq j)}^{N} g(c_{jl}) b_l,$$

for $j = 1, \ldots, N$, and

$$\frac{1}{\gamma} \partial_T b_j = \left( 1 - a_0^2 \sum_{l=1}^{N} g(c_{jl}) \right) b_j,$$

for $j = N + 1, \ldots, M$.

For parallel roll stationary solutions ($N = 1$), we have $a_0 = 1$ and

$$\frac{1}{\gamma} \partial_T b_1 = -2b_1, \quad \frac{1}{\gamma} \partial_T b_j = (1 - g(c_{1j})) b_j,$$

for $j = 2, \ldots, M$. Thus if $g(c_{1j}) < 1$ for some values of $c_{1j}$, the parallel roll stationary solution is unstable. From the $g(c_{jl})$ curves in figures 3, 4, and 5, we conclude that parallel roll stationary solutions for Faraday waves in weakly dissipative fluids are not stable.

The linear stability of square patterns ($N = 2$ and $a_0 = 1/[1 + g(0)]^{1/2}$) is determined from the following linear system:

$$\frac{1 + g(0)}{2\gamma} \partial_T b_1 = -b_1 - g(0) b_2, \quad \frac{1 + g(0)}{2\gamma} \partial_T b_2 = -b_2 - g(0) b_1,$$

$$\frac{1}{\gamma} \partial_T b_j = \left( 1 - \frac{g(c_{1j}) + g(c_{2j})}{1 + g(0)} \right) b_j,$$

for $j = 3, \ldots, M$. Thus if $-1 > g(0) > 1$ and

$$\lambda_{sq} = 1 - \frac{g(c_{1j}) + g(c_{2j})}{1 + g(0)} < 0,$$

square patterns would be stable. The first condition is satisfied as shown in figures 3, 4, and 5. Since $|c_{2j}| = (1 - c_{1j}^2)^{1/2}$, we have

$$\lambda_{sq}(c_{1j}) = 1 - \frac{g(c_{1j}) + g((1 - c_{1j}^2))^{1/2}}{1 + g(0)},$$

where $-1 \leqslant c_{1j} \leqslant 1$. The growth rate $\lambda_{sq}$ of a standing wave perturbation in an arbitrary direction to the stationary square solution is always negative except for $\Gamma_0 = 1/3$ and small values of the damping coefficient. Interestingly, this is the parameter regime for $\Gamma_0$ and $\gamma$ where hexagonal/triangular patterns are found to have lower values of the Lyapunov function than square patterns. The results of the stability analysis tell us that in this parameter range square patterns are in fact unstable, and thus correspond to a local maximum or a saddle point of the Lyapunov function. This result in turn guarantees that square patterns will not be seen in Faraday waves for this parameter range. The exact parameter range, however,

cannot be determined from the stability analysis since we are only considering a very restricted form of perturbations in the context of the SWAEs.

The linear stability of hexagonal or triangular standing wave patterns ($N = 3$ and $a_0 = 1/[1 + 2g(\frac{1}{2})]^{1/2}$) can be determined from the following linear system:

$$\frac{1 + 2g(\frac{1}{2})}{2\gamma}\partial_T b_1 = -b_1 - g(\tfrac{1}{2})(b_2 + b_3),$$

$$\frac{1 + 2g(\frac{1}{2})}{2\gamma}\partial_T b_2 = -b_2 - g(\tfrac{1}{2})(b_1 + b_3),$$

$$\frac{1 + 2g(\frac{1}{2})}{2\gamma}\partial_T b_3 = -b_3 - g(\tfrac{1}{2})(b_1 + b_2),$$

$$\frac{1}{\gamma}\partial_T b_j = \left(1 - \frac{g(c_{1j}) + g(c_{2j}) + g(c_{3j})}{1 + 2g(\frac{1}{2})}\right) b_j,$$

for $j = 4, \ldots, M$. Therefore, hexagonal or triangular patterns are unstable if $g(\frac{1}{2}) < -\frac{1}{2}$, or $g(\frac{1}{2}) > 1$ or

$$\lambda_{ht} \equiv 1 - \frac{g(c_{1j}) + g(c_{2j}) + g(c_{3j})}{1 + 2g(\frac{1}{2})} > 0,$$

for $j = 4, \ldots, M$. Similar stability analyses can also be performed for quasi-patterns ($N \geqslant 4$).

### 3.4. *Envelope equations*

We have assumed so far that Faraday wave patterns consist of a set of spatially uniform (i.e. no modulations) standing waves although we have considered the amplitude of each standing wave to be slowly varying in time. It is conceivable, however, that the standing wave amplitudes may also have slow spatial variations, i.e. standing waves with spatially modulated amplitudes. In fact, the slow spatial variations of the amplitudes can be nicely incorporated into the amplitude equations within the framework first discussed by Newell & Whitehead (1969) for pattern formation in Rayleigh–Bénard convection.

Amplitude equations including slow spatial variations of the amplitudes are often called envelope equations. In principle one can also derive a set of coupled standing wave envelope equations for parametric surface waves from the hydrodynamic equations with the assumption that spatial variations of the amplitudes are of a slow scale of the order of $\varepsilon^{1/2}$, i.e. $X = \varepsilon^{1/2}x$ and $A_j = A_j(X, T)$. With these assumptions, there will be no nonlinear terms involving spatial derivatives in the envelope equations up to $O(\varepsilon^{3/2})$ As a result, only linear terms involving spatial derivatives will appear in standing wave envelope equations, and the cubic nonlinear terms will be exactly the same as the SWAEs (3.34). The linear terms involving spatial derivatives can be obtained by a similar perturbative expansion as for the SWAEs as well as from symmetry and invariance arguments and the growth rate of the linearly unstable modes (Newell 1974; Cross & Hohenberg 1993). We have chosen the latter way, which is much simpler.

The possible scalar terms up to $O(\varepsilon^{3/2})$ are $\left(\hat{\boldsymbol{k}}_j \cdot \nabla_X\right) A_j$, $\nabla_X^2 A_j$, and $\left(\hat{\boldsymbol{k}}_j \cdot \nabla_X\right)^2 A_j$. Since the envelope equation for the standing wave amplitude $A_j$ is expected to be

---

 Nonlinear terms involving spatial derivatives would appear in the envelope equations if the SWAEs had quadratic nonlinear terms (Brandt 1989).

invariant under the transformation $\hat{\boldsymbol{k}}_j \to -\hat{\boldsymbol{k}}_j$, the first term will not appear in the equation. The second term implies the same form of the transverse and longitudinal variations for a standing wave amplitude $A_j$. Since a standing wave pattern breaks the rotational symmetry of an isotropic two-dimensional system, the transverse and longitudinal spatial variations are qualitatively different, and thus the second term also cannot appear in the envelope equations.† Therefore, we only need to consider the last term $\left(\hat{\boldsymbol{k}}_j \cdot \nabla_X\right)^2 A_j$ in the envelope equations,

$$\frac{1}{\gamma} \frac{\partial A_j}{\partial T} = A_j + \xi_0^2 \left(\hat{\boldsymbol{k}}_j \cdot \nabla_X\right)^2 A_j(X, T) - \left[|A_j|^2 + \sum_{l=1(l\neq j)}^{N} g(c_{jl})|A_l|^2\right] A_j, \qquad (3.43)$$

where $\xi_0$ is determined from the growth rate of the linearly unstable eigenmode as given by (3.5),

$$\sigma_+(k) = -\gamma + \left(f^2 - \left[(k-1)(G_0 + 3\Gamma_0)/2\right]^2\right)^{1/2}.$$

From the general arguments of Newell (1974) and Cross & Hohenberg (1993), we expand the growth rate $\sigma_+(k)$ around the critical wavenumber $k = 1$ as

$$\sigma_+(k) = \frac{1}{\tau_0} \left[\varepsilon - \xi_0^2(k-1)^2\right] + \ldots.$$

Hence we find that $\tau_0 = 1/\gamma$ and

$$\xi_0^2 = -\frac{\tau_0}{2} \left(\frac{\partial^2 \sigma_+(k)}{\partial k^2}\right)_{k=1} = \frac{\tau_0}{2f} \left(\frac{G_0 + 3\Gamma_0}{2}\right)^2 \qquad (3.44)$$

The envelope equations now can be written as:

$$\frac{1}{\gamma} \frac{\partial A_j}{\partial T} = A_j + \left(\frac{G_0 + 3\Gamma_0}{2\sqrt{2}\gamma}\right)^2 \left(\hat{\boldsymbol{k}}_j \cdot \nabla_X\right)^2 A_j - \left[|A_j|^2 + \sum_{l=1(l\neq j)}^{N} g(c_{jl})|A_l|^2\right] A_j, \qquad (3.45)$$

for $j = 1, \ldots, N$. We have set $f = \gamma$ in the spatial derivative term since the difference is of higher order.

The envelope equations (3.45) are also of gradient form

$$\frac{1}{\gamma} \frac{\partial A_j}{\partial T} = -\delta \mathscr{L}/\delta A_j^*,$$

with a Lyapunov functional

$$\mathscr{L} = \int \mathrm{d}\boldsymbol{x} \left[-\sum_{j=1}^{N} |A_j|^2 + \left|\frac{G_0 + 3\Gamma_0}{2\sqrt{2}\gamma} \left(\hat{\boldsymbol{k}}_j \cdot \nabla_X\right) A_j\right|^2 \right.$$
$$\left. + \frac{1}{2} \sum_{j=1}^{N} |A_j|^2 \left(|A_j|^2 + \sum_{l=1(l\neq j)}^{N} g(c_{jl})|A_l|^2\right)\right]. \qquad (3.46)$$

† With the assumption of different slow spatial scales for the transverse and longitudinal modulations in analogy to Rayleigh–Bénard convection, scalar terms of the following form are permissible in standing wave amplitude equations: $\left[\hat{\boldsymbol{k}}_j \cdot \nabla_X - (\mathrm{i}/2) \left(\hat{\boldsymbol{k}}_j^\perp \cdot \nabla_X\right)^2\right]^2 A_j$ with $\hat{\boldsymbol{k}}_j^\perp$ a unit vector perpendicular to $\hat{\boldsymbol{k}}_j$. We do not consider such terms here since we are only computing the coherence length $\xi_0$ in the longitudinal direction. The more general case of transverse modulations has been explicitly addressed by Zhang (1994).

An important point about the standing wave envelope equations (3.45) and the Lyapunov functional (3.46) is that the coefficient of the spatial derivative term is much greater than one, i.e.

$$\xi_0 = \frac{G_0 + 3\Gamma_0}{2\sqrt{2}\gamma} \gg 1, \tag{3.47}$$

since $\gamma \ll 1$ for weakly dissipative surface waves. Physically $\xi_0$ is a measure of the coherence length of the wave pattern. Thus (3.47) implies that standing wave patterns of Faraday waves in weakly dissipative fluids have a coherence length much longer than their wavelength. This should be compared to Rayleigh–Bénard convection, where we have $\xi_0 \sim 1$ (Newell & Whitehead 1969; Cross & Hohenberg 1993), and to directional solidification of a binary alloy, where $\xi_0 \ll 1$ due to the extremely flat neutral stability curve (Mullins & Sekerka 1964). Because $\xi_0 \gg 1$, highly ordered square patterns as large as $30 - 40$ wavelengths are often observed in Faraday waves in weakly viscous fluids (Gaponov-Gerkhov & Rabinovich 1990).

## 4. Summary and discussion

We have studied pattern formation in weakly damped Faraday waves by deriving a set of linear damping quasi-potential equations and by performing a multiscale asymptotic expansion close to onset. Standing wave equations have been derived that explicitly incorporate higher-harmonic terms in the linear neutral solutions. These terms are seen to be important for the saturation of the wave amplitude (amplitude-limiting effect by the driving force). We have also studied in detail the effect of triad resonant interactions among capillary–gravity waves on nonlinear pattern selection. Triad resonant interactions are found to be the main reason for the appearance of square patterns in capillarity-dominated Faraday waves. By increasing the gravity wave component, the triad resonant condition is altered. As a result, square patterns can become unstable, and hexagonal or quasi-crystalline patterns can be stabilized.

The importance of higher-harmonic terms in the linear neutral solutions also has implications for parametric surface waves in highly viscous fluids. Because of the larger threshold values of the driving force for highly viscous fluids, higher-harmonic terms in the linear neutral solutions can be even more important than in the weakly damped case considered here. More than one higher-harmonic term can be important in that case.

Our results provide justification for the observed selected patterns of square symmetry near onset in fluids of low viscosity (Lang 1962; Ezerskii *et al.* 1985; Tufillaro *et al.* 1989; Ciliberto *et al.* 1991; Bosch & van de Water 1993; Edwards & Fauve 1993; Müller 1993). Without requiring any additional assumptions, Faraday waves close to onset are potential, and minimization of the associated Lyapunov functional leads to square patterns in the capillarity-dominated regime. This is in agreement with most experimental studies, with the exception of the work by Christiansen, Alstrøm & Levinsen (1995) who observed quasi-patterns where we predict squares. More recently, a systematic survey of pattern selection in a system of large aspect ratio by Kudrolli & Gollub (1996) has again documented the transition to squares for capillary-dominated waves, but also shown the transition to hexagons in the vicinity of $\Gamma = 1/3$, in agreement with our predictions. In the range in which we predict stable quasi-patterns, Kudrolli & Gollub (1996) observe hexagons instead. The origin of this discrepancy remains to be investigated.

## REFERENCES

BANERJEE, P. P. & KORPEL, A. 1982 *Phys. Fluids* **25**, 1938.

BATCHELOR, G. K. 1967 *An Introduction to Fluid Dynamics*. Cambridge University Press.

BECHHOEFER, J., EGO, V., MANNEVILLE, S. & JOHNSON, B. 1995 *J. Fluid Mech.* **288**, 325.

BENJAMIN, T. B. & URSELL, F. 1954 *Proc. R. Soc. Lond.* A **225**, 505.

BOSCH, E., LAMBERMONT, H. & WATER, W. VAN DE 1994 *Phys. Rev.* E **49**, R3580.

BOSCH, E. & WATER, W. VAN DE 1993 *Phys. Rev. Lett.* **70**, 3420.

BRANDT, H. R. 1989 *Prog. Theor. Phys. Suppl.* **99**, 442.

BRIDGER, J., GLUCKMAN, B. J., MARCQ, P. & GOLLUB, J. P. 1993 *Phys. Rev. Lett.* **71**, 2034.

CHRISTIANSEN, B., ALSTRØM, P. & LEVINSEN, M. T. 1992 *Phys. Rev. Lett.* **68**, 2157.

CHRISTIANSEN, B., ALSTRØM, P. & LEVINSEN, M. T. 1995 *J. Fluid Mech.* **291**, 323.

CILIBERTO, S., DOUADY, S. & FAUVE, S. 1991 *Europhys. Lett.* **15**, 23.

CRAIG, W. 1989 In *Proc. IMA Workshop on Nonlinear Microlocal Analysis* (ed. M. Beals). Springer.

CRAIG, W. & SULEM, C. 1993 *J. Comput. Phys.* **108**, 73.

CRAIK, A. D. D. 1985 *Wave Interactions and Fluid Flows*. Cambridge University Press.

CROSS, M. C. 1980 *Phys. Fluids* **23**, 1727.

CROSS, M. C. & HOHENBERG, P. C. 1993 *Rev. Mod. Phys.* **65**, 851.

DAUDET, L., EGO, V., MANNEVILLE, S. & BECHHOEFER, J. 1995 *Europhys. Lett.* **32**, 313.

DOUADY, S. 1990 *J. Fluid Mech.* **221**, 383.

EDWARDS, W. S. & FAUVE, S. 1993 *Phys. Rev.* E **47**, 123.

EDWARDS, W. S. & FAUVE, S. 1994 *J. Fluid Mech.* **278**, 123.

EZERSKII, A. B., KOROTIN, P. I. & RABINOVICH, M. I. 1985 *Zh. Eksp. Teor. Fiz.* **41**, 129 (transl. 1986 *Sov. Phys. JETP* **41**, 157).

FARADAY, M. 1831 *Phil. Trans. R. Soc. Lond.* **52**, 319.

FAUVE, S., KUMAR, K., LAROCHE, C., BEYSENS, D., & GARRABOS, Y 1992 *Phys. Rev. Lett.* **68**, 3160.

GAPONOV-GREKHOV, A. V. & RABINOVICH, M. I. 1990 *Physics Today* July, 30.

GOLLUB, J. P. & RAMSHANKAR, R. 1991 In *New Perspectives in Turbulence* (ed. L. Sirovich), p. 165. Springer.

GOLUBITSKY, M., SWIFT, J. W. & KNOBLOCH, E. 1984 *Physica* D **10**, 249.

HAMMACK, J. L. & HENDERSON, D. M. 1993 *Ann. Rev. Fluid Mech.* **25**, 55.

HOGAN, S. J. 1984 *Phys. Fluids* **27**, 42.

KUDROLLI, A. & GOLLUB, J. P. 1996 Patterns and spatiotemporal chaos in parametrically forced surface waves: a systematic survey at large aspect ratio. *Physica* D **97**, 133.

KUMAR, K. & TUCKERMAN, L. S. 1994 *J. Fluid Mech.* **279**, 49.

LAMB, H. 1932 *Hydrodynamics*. Cambridge University Press.

LANDAU, L. D. & LIFSHITZ, E. M. 1959 *Fluid Mechanics*. Pergamon.

LANG, R. J. 1962 *J. Acoust. Soc. Am.* **34**, 6.

LUNDGREN, T. S. 1989 In *Mathematical Aspects of Vortex Dynamics* (ed. R. S. Caflisch). SIAM, Philadelphia.

LUNDGREN, T. S. & MANSOUR, N. N. 1988 *J. Fluid Mech.* **194**, 479.

MALOMED, B. A., NEPOMNYASHCHIĬ, A. A. & TRIBELSKIĬ, M. I. 1989 *Sov. Phys. JETP* **69**, 388.

McGOLDRICK, L. F. 1970 *J. Fluid Mech.* **40**, 251.

MILDER, D. M. 1977 *J. Fluid Mech.* **83**, 159.

MILES, J. W. 1967 *Proc. R. Soc. Lond.* A **297**, 459.

MILES, J. W. 1977 *J. Fluid Mech.* **83**, 153.

MILES, J. W. 1984 *J. Fluid Mech.* **146**, 285.

MILES, J. W. 1993 *J. Fluid Mech.* **248**, 671.

MILES, J. W. 1994 *J. Fluid Mech.* **69**, 353.

MILES, J. W. & HENDERSON, D. 1990 *Ann. Rev. Fluid Mech.* **22**, 143.

MILNER, S. T. 1991 *J. Fluid Mech.* **225**, 81.

MÜLLER, H. W. 1993 *Phys. Rev. Lett.* **71**, 3287.

MULLINS, W. W. & SEKERKA, R. F. 1964 *J. Appl. Phys.* **35**, 444.

NEWELL, A. C. 1974 In *Nonlinear Wave Motion* (ed. A. C. Newell). Lectures in Applied Mathematics Vol. 15. Am. Math. Soc., Providence.

NEWELL, A. C., PASSOT, T. & LEGA, J. 1993 *Ann. Rev. Fluid Mech.* **25**, 399.

NEWELL, A. C. & WHITEHEAD, J. A. 1969 *J. Fluid Mech.* **38**, 279.

RAYLEIGH, LORD 1883 *Phil. Mag.* **16**, 50.

RUVINSKY, K. D., FELDSTEIN, F. I. & FREIDMAN, G. I. 1991 *J. Fluid Mech.* **230**, 339.

RUVINSKY, K. D. & FREIDMAN, G. I. 1985 In *IX All-Union Symp. on Diffraction and Propagation Waves. Theses of Reports*, Vol. 2 Tbilisi.

SEGEL, L. A. 1969 *J. Fluid Mech.* **38**, 203.

SHECHTMAN, D. S., BLECH, I., GRATIAS, D. & CAHN, J.W. 1984 *Phys. Rev. Lett.* **53**, 1951.

TUFILLARO, N. B., RAMSHAMKAR, R. & GOLLUB, J. P. 1989 *Phys. Rev. Lett.* **62**, 422.

WHITHAM, G. B. 1974 *Linear and Nonlinear Waves*. Wiley.

WILTON, J. R. 1915 *Phil. Mag.* **29**(6), 688.

YUEN, H. C. & LAKE, B. M. 1982 In *Advances in Applied Mechanics* (ed. C.-S. Yih). Academic.

ZAKHAROV, V. E. 1968 *Zh. Prikl. Mekh. Tekh. Fiz.* **9**, 86 (transl. 1968 *J. Appl. Mech. Tech. Phys.* **9**, 190).

ZAKHAROV, V. E., L'VOV, V. S. & STAROBINETS, S. S. 1975 *Usp. Fiz. Nauk.* **114**, 609 (transl. (1975) *Sov. Phys. Usp.* **17**, 896).

ZHANG, W. 1994 Pattern formation in weakly damped parametric surface waves. PhD thesis, Florida State University.

ZHANG, W. & VIÑALS, J. 1996 *Phys. Rev.* E **53**, R4283.